


# Soybean MKK2 establishes intricate signalling pathways to regulate soybean response to cyst nematode infection

Tracy E. Hawk | Sarbottam Piya | Mst Shamira Sultana | Sobhan Bahrami Zadegan | Sarah Shipp | Nicole Coffey | Natalie B. McBride | John H. Rice | Tarek Hewezi 

Department of Plant Sciences, University of Tennessee, Knoxville, Tennessee, USA

## Correspondence

Tarek Hewezi, Department of Plant Sciences, University of Tennessee, Knoxville, TN 37996, USA.  
Email: [thewezi@utk.edu](mailto:thewezi@utk.edu)

## Funding information

USDA-NIFA, Grant/Award Number: 2018-67013-27822

## Abstract

Mitogen-activated protein kinase (MPK) cascades play central signalling roles in plant immunity and stress response. The soybean orthologue of MPK kinase2 (GmMKK2) was recently identified as a potential signalling node whose expression is upregulated in the feeding site induced by soybean cyst nematode (SCN, *Heterodera glycines*). To investigate the role of GmMKK2 in soybean-SCN interactions, we overexpressed a catabolically inactive variant referred to as kinase-dead variant (KD-GmMKK2) using transgenic hairy roots. KD-GmMKK2 overexpression caused significant reduction in soybean susceptibility to SCN, while overexpression of the wild-type variant (WT-GmMKK2) exhibited no effect on susceptibility. Transcriptome analysis indicated that KD-GmMKK2 overexpressing plants are primed for SCN resistance via constitutive activation of defence signalling, particularly those related to chitin, respiratory burst, hydrogen peroxide and salicylic acid. Phosphoproteomic profiling of the WT-GmMKK2 and KD-GmMKK2 root samples upon SCN infection resulted in the identification of 391 potential targets of GmMKK2. These targets are involved in a broad range of biological processes, including defence signalling, vesicle fusion, chromatin remodelling and nuclear organization among others. Furthermore, GmMKK2 mediates phosphorylation of numerous transcriptional and translational regulators, pointing to the presence of signalling shortcuts besides the canonical MAPK cascades to initiate downstream signalling that eventually regulates gene expression and translation initiation. Finally, the functional requirement of specific phosphorylation sites for soybean response to SCN infection was validated by overexpressing phospho-mimic and phospho-dead variants of two differentially phosphorylated proteins SUN1 and IDD4. Together, our analyses identify GmMKK2 impacts on signalling modules that regulate soybean response to SCN infection.

## KEYWORDS

defence responses, mitogen-activated protein kinases, phosphoproteomics, RNA-seq, soybean, soybean cyst nematode

This is an open access article under the terms of the [Creative Commons Attribution-NonCommercial-NoDerivs](https://creativecommons.org/licenses/by-nc-nd/4.0/) License, which permits use and distribution in any medium, provided the original work is properly cited, the use is non-commercial and no modifications or adaptations are made.

© 2024 The Authors. *Molecular Plant Pathology* published by British Society for Plant Pathology and John Wiley & Sons Ltd.

## 1 | INTRODUCTION

Plants have evolved an effective and robust two-tiered immune system to protect them from most pathogens. Cell surface receptors recognize conserved molecular structures on the surfaces of groups of related microbes, referred to as pathogen/microbe-associated molecular patterns (PAMPs or MAMPs) that trigger the first layer of plant response known as pathogen-triggered immunity (PTI) (Zhou & Zhang, 2020). PTI is efficient at disrupting invasion from non-adapted pathogens; however, some pathogens are able to evade PTI using an array of effector proteins that they secrete into plant cells to modify the host response. In turn, plants have evolved nucleotide oligomerization domain (NOD)-like receptors that directly or indirectly recognize effector proteins and activate effector-triggered immunity (ETI) (Wu et al., 2017). However, activation of such a response is often at the expense of plant growth and development (He et al., 2022). Therefore, activation of immune responses such as induction of reactive oxygen species (ROS) and salicylic acid signalling is under tight regulation by many different signalling pathways (Liu et al., 2016; Withers & Dong, 2017).

Mitogen-activated protein kinases (MPKs) are important nodes that convert external environmental signals into intracellular responses through activation of MPK cascades. Generally speaking, MPK cascades are triggered by plasma membrane receptors, which phosphorylate MAPK kinase kinases (MAPKKKs). The activated MAPKKKs phosphorylate MAPK kinases (MKKs), which in turn activate MPKs (Rodriguez et al., 2010; Widmann et al., 1999). MAPKs ultimately activate downstream transcription factors, enzymes, or other protein kinases to trigger appropriate cellular responses to external stimuli (Zhang et al., 2018). MPK cascades can be activated in response to environmental stresses such as extreme heat, drought and salinity (Moustafa et al., 2014) as well as upon recognition of invading pathogens (Meng & Zhang, 2013). Recognition of pathogen effectors or PAMPs activates pathogen-responsive MAPK cascades leading to phosphorylation of downstream target proteins involved in a broad range of defence response including biosynthesis of defence hormones and antimicrobial metabolites, strengthening of the plant cell wall, production of ROS and activation of defence genes and the hypersensitive response (HR) (Meng & Zhang, 2013; Pitzschke, Schikora, et al., 2009; Withers & Dong, 2017; Zhang et al., 2018).

The complexity of the MAPK cascade signalling is demonstrated by the differential binding ability of individual MAPKs to numerous targets together with the potential combinatorial assembly of these kinases and their involvement in various programmes of plant growth and development and stress responses (Hamel et al., 2006; He et al., 2020; Meng & Zhang, 2013; Tena et al., 2001, 2011; Zhang et al., 2018). MPK3, MPK4 and MPK6 are among the most extensively studied MPKs involved in innate immunity (Asai et al., 2002; Park et al., 2021; Pitzschke, Djamei, et al., 2009; Pitzschke, Schikora, et al., 2009; Völz et al., 2022; Xu et al., 2016; Zhang et al., 2012; Zou et al., 2021). MPK4 is involved

in plant growth, development and cytokinesis as well as innate immunity and defence responses (Pitzschke, Djamei, et al., 2009). The MPK4 cascade is triggered by the perception of PAMPs by PAMP receptors upstream of MAPK kinase kinase 1 (MEKK1) (Gao et al., 2008). Upon activation, MEKK1 phosphorylates MKK1/MKK2, which function redundantly and activate MPK4 (Ichimura et al., 2006; Nakagami et al., 2006; Qiu et al., 2008; Suarez-Rodriguez et al., 2006). The MEKK1, MKK1/MKK2 and MPK4 cascade is activated during PTI and is thought to negatively regulate the plant defence response (Berriri et al., 2012; Brodersen et al., 2006; Liu et al., 2011; Petersen et al., 2000; Zhang et al., 2012). Loss-of-function mutations of *MEKK1*, *MKK1/2* and *MPK4* results in constitutive induction of salicylic acid-mediated defence, enhanced resistance to pathogens and stunted growth (Gao et al., 2008; Ichimura et al., 2006; Nakagami et al., 2006; Suarez-Rodriguez et al., 2006), supporting a negative regulatory function of this cascade in plant immunity. However, other studies have shown a role of MKK2 signalling cascade in positively regulating some aspects of plant defence in Arabidopsis. For example, plants constitutively overexpressing *MKK2* displayed enhanced resistance to the bacterial pathogens *Pseudomonas syringae* and *Erwinia carotovora* (Brader et al., 2007), whereas knockout of *MKK2* resulted in increased susceptibility to *Phytophthora parasitica* (Li et al., 2022). The current understanding is that several nucleotide-binding leucine-rich repeat (NB-LRR) proteins are monitoring the integrity of this cascade and activate a defence response upon disruption (Takagi et al., 2018; Zhang et al., 2012, 2017).

In soybean, the MEKK1-MKK1/MKK2-MPK4 signalling cascade has been reported to negatively regulate defence signalling. Silencing of *GmMEKK1* and *GmMPK4* results in constitutive activation of immunity-related genes. However, silencing of *GmMCK1/GmMCK2* has no effect (Liu et al., 2011; Xu et al., 2018). The authors attributed this phenotype to functional redundancy among *GmMCK* homologues and insufficient co-silencing of *GmMCK1* and *GmMCK2*. To date, the downstream components of this cascade and the mechanism underlying immunity and defence gene expression regulation remain poorly understood.

The soybean cyst nematode (SCN, *Heterodera glycines*) is an economically important root parasite of soybean plants that causes dramatic yield loss worldwide. This sedentary endoparasite forms a sophisticated feeding site within the root vascular tissues called the syncytium, which provides the infective juveniles with all necessary nourishment to complete their life cycle (Hewezi & Baum, 2017; Kyndt et al., 2013). When the infective second-stage juvenile (J2) identifies a compatible cell, sequential cell-to-cell fusion events of hundreds of surrounding cells are rapidly initiated leading to the formation of large multinucleated syncytium. These cell-to-cell fusion events are also accompanied by physiological and structural cellular reorganizations, including cell wall modifications, increased cytoplasm density, fragmentation of large vacuoles, endoreduplication, hypertrophy of nuclei and nucleoli and increased abundance of organelles required for the enhanced metabolic activity of these feeding cells (Siddique &

Grundler, 2015; Smant et al., 2018; Sobczak & Golinowski, 2011). A growing body of studies indicate that reprogramming of root cells into syncytium cell type involves the action of major regulators such as transcription factors, microRNAs and kinase signalling nodes (Hawk et al., 2023; Hwezi, 2020; Hwezi et al., 2015; Mejias et al., 2019; Mendy et al., 2017; Piya et al., 2017; Siddique & Grundler, 2018). However, despite the establishment of MAPKs as regulators of multiple signalling systems, the function of these conserved signalling molecules in plant–nematode interactions remains very limited. The only functional study reported was on the positive role of MPK3 and MPK6 in enhancing plant immunity against the beet cyst nematode *Heterodera schachtii* (Sidonskaya et al., 2016).

Recently, we have identified soybean MKK2 (GmMKK2) as a potential signalling node in the SCN-induced syncytium (Piya et al., 2022). In this study, we investigated the function of GmMKK2 in establishing the SCN–soybean interactions. We revealed that GmMKK2 is involved, as a negative regulator, in an intricate network of defence signalling and interactions with other MAPK components, transforming pathogen signal into cellular responses to mediate SCN susceptibility. In addition, a substantial number of GmMKK2's putative substrates were identified using a quantitative phosphoproteomic approach. Together, our results provide intriguing insights into the mechanisms through which GmMKK2 initiates downstream signalling that ultimately regulates gene expression and potentially translation initiation.

## 2 | RESULTS

### 2.1 | GmMKK2 is a nucleocytoplasmic protein

To determine the subcellular localization of GmMKK2 (Glyma.13G106900), the coding sequence of the wild-type GmMKK2 (WT-GmMKK2) was fused to the N terminus of an enhanced cyan fluorescent protein (eCFP) and agroinfiltrated into *Nicotiana benthamiana* leaves. CFP signals were detected in both cytoplasm and nucleus (Figure 1a). To determine whether the kinase activity of GmMKK2 has an effect on protein localization, we generated and determined the subcellular localization of a catabolically inactive variant referred to as kinase-dead variant (KD-GmMKK2). This kinase-dead variant was constructed by mutating the conserved lysine residues at the ATP and substrate-binding sites (K99 and K194), to arginine as recently described (Hawk et al., 2023; Piya et al., 2022) (Figure S1). Similar to WT-GmMKK2:eCFP, the KD-GmMKK2:eCFP fusion exhibited nucleocytoplasmic localization (Figure 1a). In addition, the intensity of the CFP signal of both constructs was very comparable. This localization pattern is in accord with earlier studies in *Arabidopsis* and soybean (Gao et al., 2008; Liu et al., 2011) and indicates that the kinase-dead mutation had no macroscopic effect on protein localization in the heterologous *N. benthamiana* overexpression system.

### 2.2 | GmMKK2 expression is upregulated during the early stages of SCN infection

We quantified transcript abundance of GmMKK2 during various stages of SCN infection using reverse transcription-quantitative PCR (RT-qPCR). Three-day-old seedlings of Williams 82 (SCN-susceptible cultivar) were inoculated with second-stages juveniles (J2s) of SCN. Syncytium-enriched tissues were collected in three biological replicates at 3, 5, 7 and 14 days post-inoculation (dpi). At each time point, whole roots were harvested from non-infected plants and used as control. GmMKK2 transcript abundance was significantly upregulated at 3 and 5 dpi compared to the corresponding non-infected root tissues (Figure 1b). However, at 7 and 14 dpi, GmMKK2 expression was significantly downregulated. The upregulation of GmMKK2 at the early time points suggests a role in suppressing basal immunity during syncytium initiation and formation stages.

### 2.3 | Overexpression of the catabolically inactive variant of GmMKK2 dramatically reduced soybean susceptibility to SCN

To examine the potential involvement of GmMKK2 in establishing soybean susceptibility to SCN, we generated composite plants with transgenic hairy roots overexpressing either WT-GmMKK2 or KD-GmMKK2 in Williams 82 background. Transgenic hairy roots expressing the empty binary vector were also generated and included as control. The transgenic hairy roots of WT-GmMKK2 or KD-GmMKK2 plants did not exhibit any morphological changes when compared with those expressing the empty vector. The expression of GmMKK2 was quantified in three biological samples of randomly selected GFP-positive roots to confirm the functionality of the overexpression constructs. GmMKK2 in wild-type and kinase-dead hairy roots showed comparable overexpression levels ranging between 3- and 13-fold across various biological samples relative to the control roots. Five weeks after inoculation, cysts were harvested from each plant independently and counted in order to determine cyst index as a percentage of cyst counts determined on control plants. Overexpression of WT-GmMKK2 resulted in a non-significant 25% increase in cyst index (Figure 2a,b). However, overexpression of KD-GmMKK2 resulted in a dramatic increase in plant resistance to SCN with 87% reduction in cyst index (Figure 2c,d). This suggests that GmMKK2 is a component of a signalling cascade that is important for the compatible interaction between soybean and SCN.

### 2.4 | GmMKK2 negatively regulates soybean defence signalling

In order to determine the impact that GmMKK2 had on the root transcriptome, we performed RNA-seq analysis with root tissues

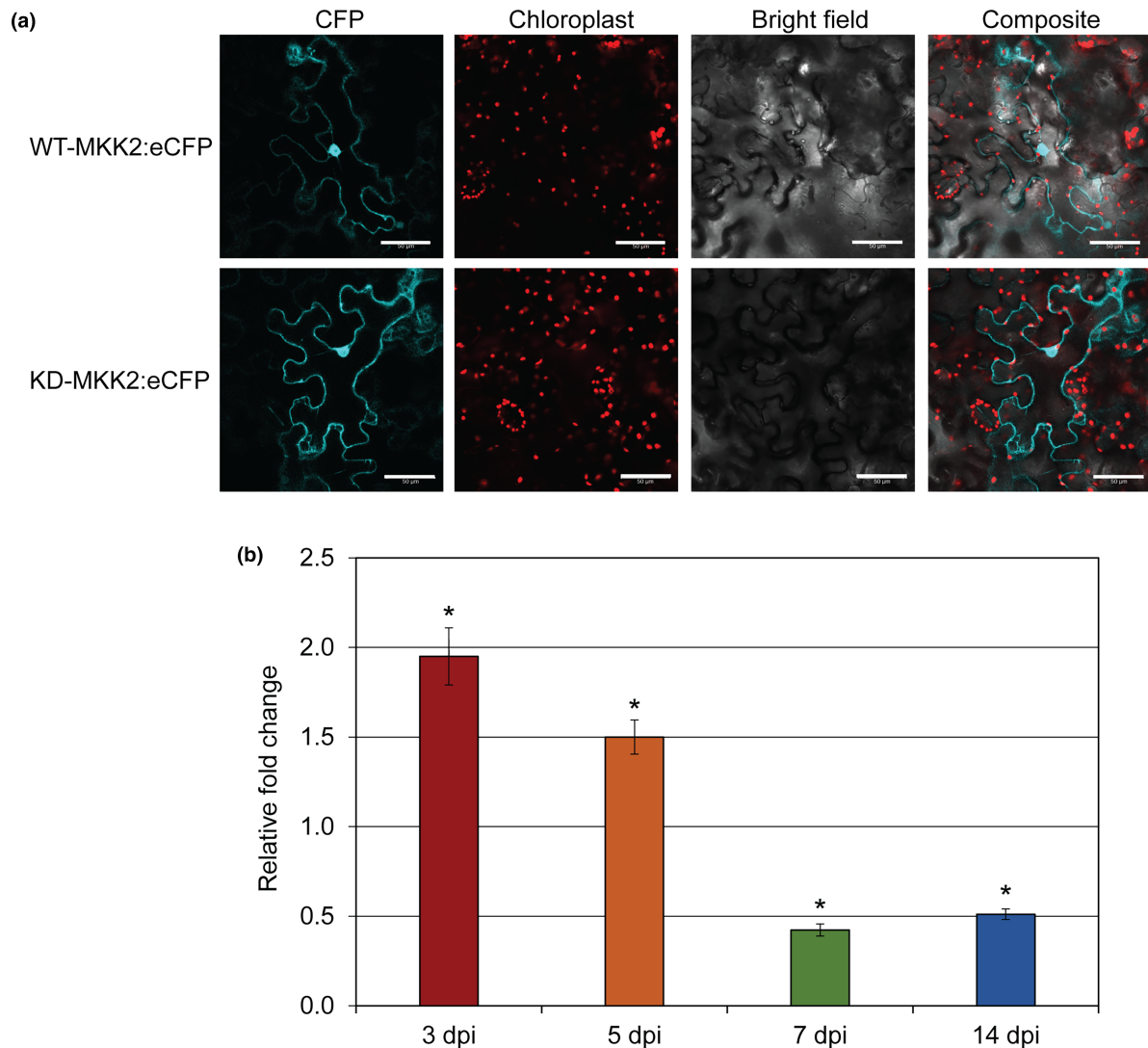


**FIGURE 1** Subcellular localization and expression patterns of GmMKK2 in response to soybean cyst nematode (SCN) infection. (a) Nucleocytoplasmic localization of wild-type (WT)-GmMKK2 and kinase-dead (KD)-GmMKK2. The coding sequences of WT-GmMKK2 and KD-GmMKK2 were fused to the N terminus of enhanced cyan fluorescent protein (eCFP) and introduced into *Nicotiana benthamiana* leaves using agroinfiltration. Fluorescence was determined approximately 24 h after agroinfiltration. Scale bar = 50  $\mu$ m. (b) Upregulation of GmMKK2 during early stage of SCN infection. The expression level of GmMKK2 was quantified in Williams 82 in response to SCN using reverse transcription-quantitative PCR. Whole non-infected root tissues (control) and syncytium-enriched root tissues were collected at 3, 5, 7 and 14 days post-inoculation (dpi) with SCN. Bars represent average  $\pm$  SE values, which were calculated using three biological replicates, each with two technical replicates. Differences in expression levels of GmMKK2 in syncytium-enriched root samples and control, which was set to 1, were analysed using *t* tests, with asterisks indicating statistically significant differences ( $p < 0.05$ ).

overexpressing either WT-GmMKK2, KD-GmMKK2, or the empty vector (control) under non-infected and infected conditions. Composite plants were generated for each genotype and inoculated with freshly hatched J2s of SCN HG Type 0. Root tissues were collected in three biological samples from both infected and the corresponding non-infected control plants at 5 dpi. In non-infected WT-GmMKK2 samples, 3422 upregulated genes and 5316 downregulated genes were identified when compared with control root samples (Table S1). Gene ontology (GO) analysis showed significant over-representation for genes involved in the transport of nitrate, ion, cation, amino acid and lipid among the upregulated genes. This finding is consistent with increasing

molecule transport across the plasma membrane during the compatible interaction (Hammes et al., 2005; Siddique et al., 2022). In accordance with GmMKK2 function, terms associated with MAPK cascade and regulation of protein dephosphorylation were also enriched among the upregulated genes (Figure 3a). The downregulated genes were enriched in GO categories associated with various aspects of cell wall modifications, oxidation-reduction, regulation of meristem initiation and growth and microtubule-based movement (Figure 3a).

Similarly, we compared KD-GmMKK2 overexpressing root samples with control samples under non-infected conditions and identified 2344 upregulated genes and 3641 downregulated genes



**FIGURE 2** Overexpression of catabolically inactive variant of *GmMCK2* greatly reduced soybean susceptibility to soybean cyst nematodes (SCN). Wild-type (*WT*)-*GmMCK2* and kinase-dead (*KD*)-*GmMCK2* were overexpressed in the SCN-susceptible cultivar Williams 82 using the transgenic hairy root system. Composite plants were inoculated with approximately 2500 eggs of SCN and 5 weeks after inoculation, cysts were isolated, counted and used to calculate cyst indexes. (a, b) Cyst counts (a) and cyst index (b) of *WT-GmMCK2* overexpression plants showing slight non-significant increase in SCN susceptibility. (c, d) Cyst counts (c) and cyst index (d) of *KD-GmMCK2* overexpression plants showing significant decrease in SCN susceptibility compared the control plants overexpressing the empty vector. Statistically significant differences were calculated using analysis of variance ( $p < 0.05$ ) and indicated with an asterisk.

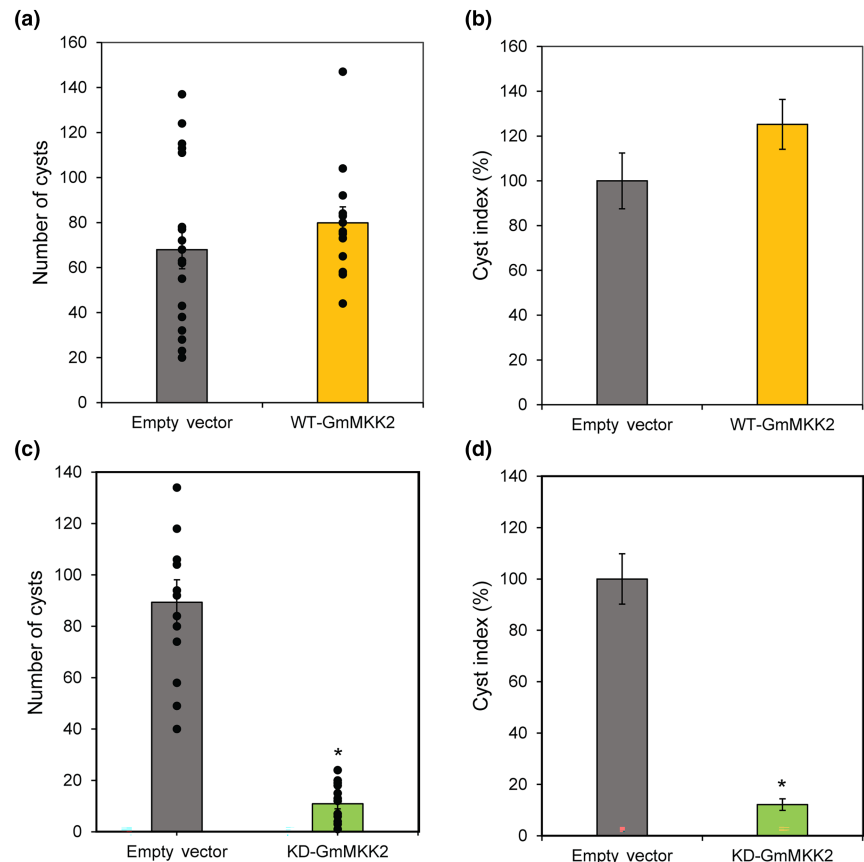


(Table S2). Interestingly, GO terms associated with defence responses and immune system regulation were predominantly enriched among the upregulated genes (Figure 3b), a finding that is consistent with increased SCN resistance in the *KD-GmMCK2* overexpression plants. In contrast, GO terms related to various developmental processes and organ patterning and specification were the most enriched among downregulated genes (Figure 3b).

## 2.5 | Wild-type and kinase-dead variants of *GmMCK2* induced distinct transcriptome reprogramming in response to SCN infection

We next examined the impacts of *WT-GmMCK2* and *KD-GmMCK2* on gene expression in response to SCN infection. SCN infection induced upregulation of 1210 genes and downregulation of 1213 genes in *WT-GmMCK2* root samples as compared to non-infected root samples (Table S3). In SCN-infected *KD-GmMCK2* samples versus non-infected samples, we identified 636 upregulated genes and 637 downregulated genes (Table S4). Venn diagram analysis of up- and downregulated genes in these two genotypes indicated that the large majority of the genes are uniquely upregulated or downregulated in a single genotype with only 218 genes (146+72) being similarly regulated in both genotypes (Figure 4a). These results indicate that wild-type and kinase-dead variants of *GmMCK2* induce distinct transcriptome reprogramming after SCN infection. The exclusively upregulated genes in SCN-infected *WT-GmMCK2* samples

were enriched in various GO categories linked to nematode parasitism, including responses to wounding, chitin and hormone stimuli, oxidation-reduction process, hormone biosynthesis and signalling pathways and defence response (Figure 4b), whereas the exclusively downregulated genes were enriched in GO categories related to lipid transport, cell wall modifications, regulation of growth rate and pattern specification process (Figure 4b). The exclusively upregulated genes in SCN-infected *KD-GmMCK2* samples were enriched in a number of GO terms associated with defence response (response to chitin, respiratory burst and salicylic acid-mediated signalling pathway), whereas the downregulated genes were enriched in genes involved in maltose biosynthetic process. These data imply that activation of defence-responsive genes and suppression of sucrose metabolic genes upon SCN infection contribute to SCN resistance in *KD-GmMCK2* overexpressing plants.

## 2.6 | Phosphoproteomic profiles of *WT-GmMCK2* and *KD-GmMCK2* plants under non-infected conditions

To better understand how *GmMCK2* contributes to plant susceptibility to SCN and identify potential downstream targets, a quantitative phosphoproteomic analysis was performed. Transgenic hairy roots overexpressing either *WT-GmMCK2*, *KD-GmMCK2*, or the empty vector (control) under both SCN-infected and non-infected conditions were collected in three biological samples and used.

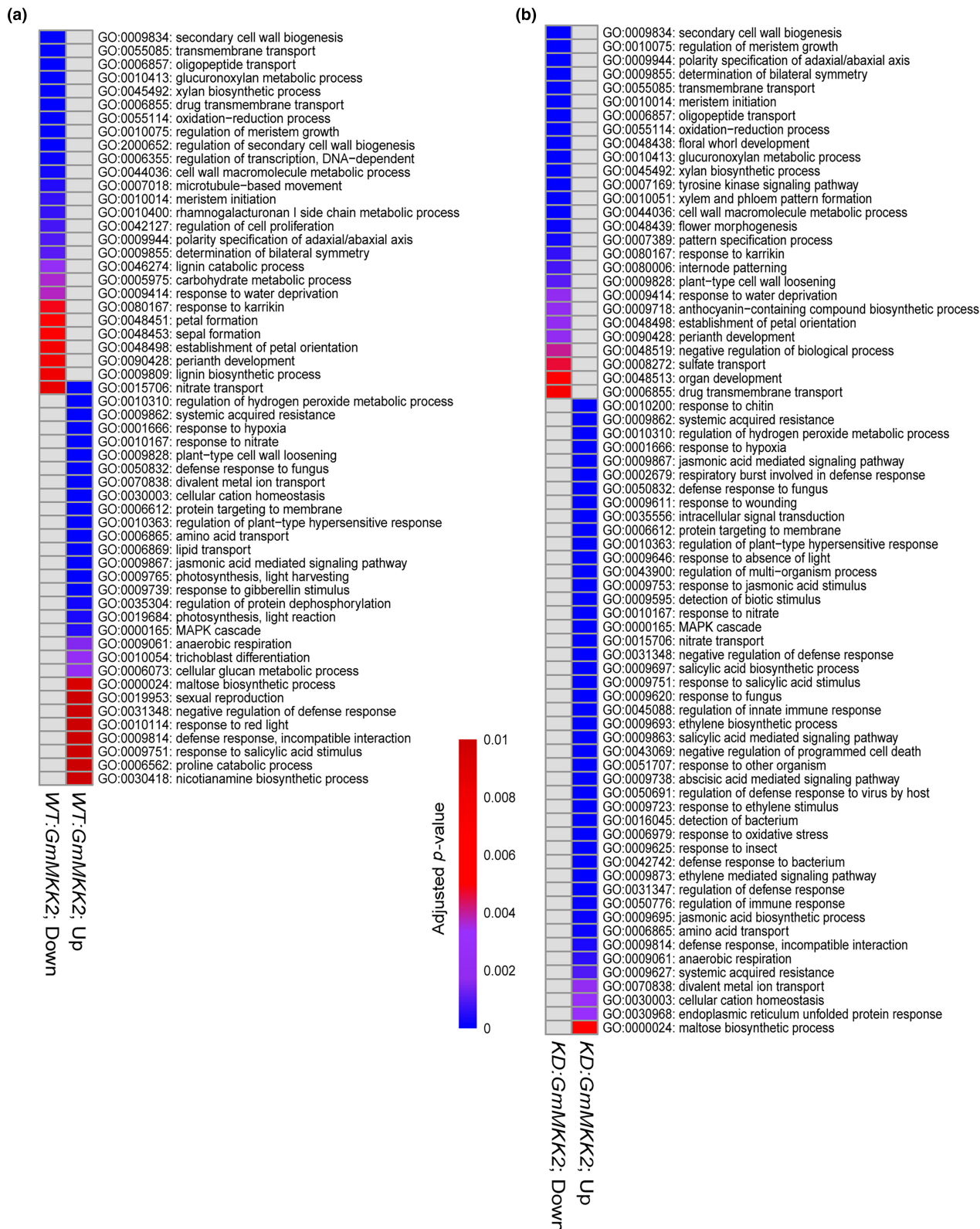
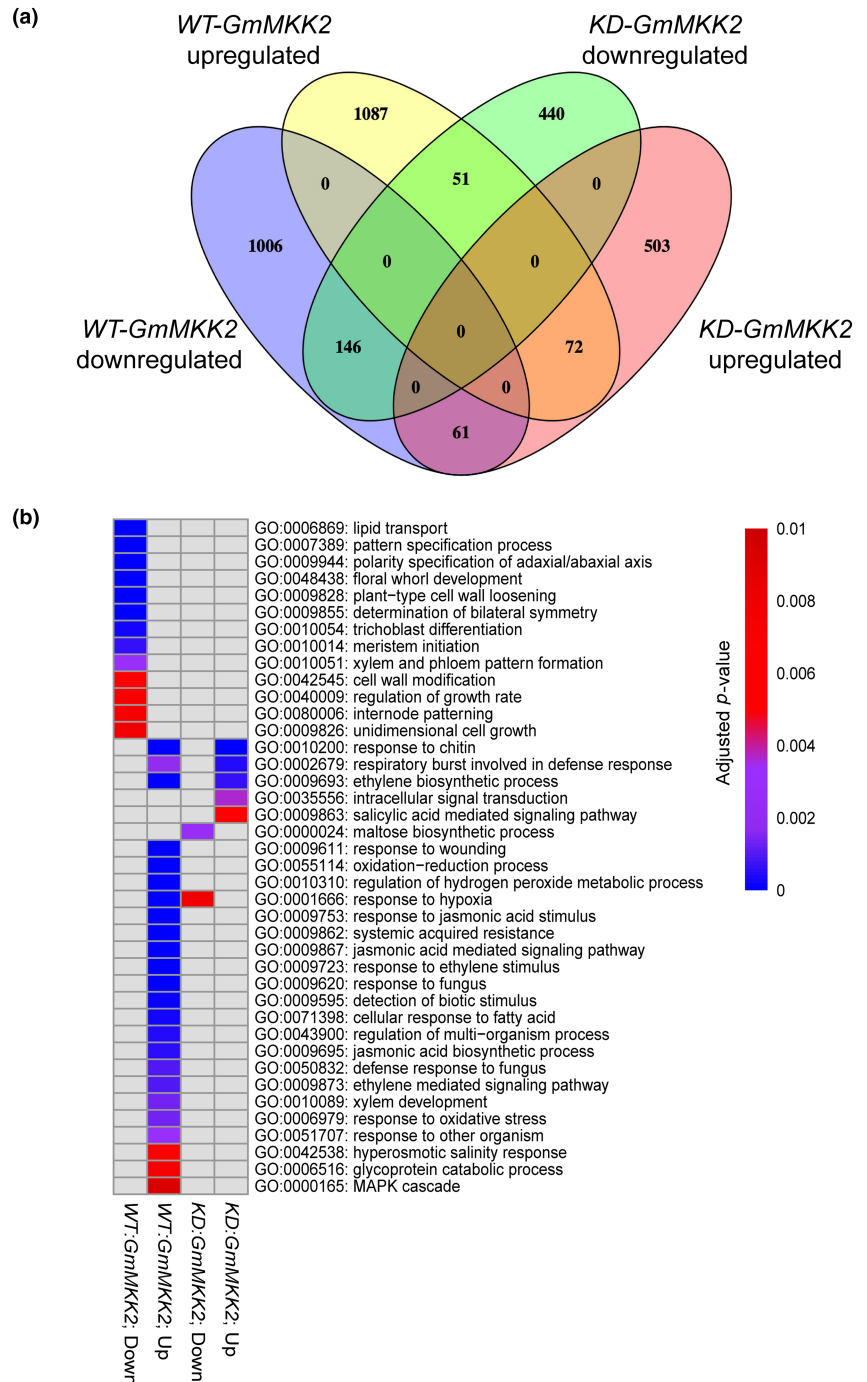


**FIGURE 3** Heat map representation of significantly enriched gene ontology (GO) terms among upregulated and downregulated genes determined in root tissues of wild-type (WT)-*GmMCK2* and kinase-dead (KD)-*GmMCK2* plants under non-infected conditions. (a, b) Significantly upregulated (up) and downregulated (down) genes were determined in root tissues of WT-*GmMCK2* (a) and KD-*GmMCK2* (b) plants in comparison with control plants expressing the empty vectors under non-infected conditions. Significantly enriched GO terms (adjusted *p*-value <0.01) were identified using the SoyBase (<https://soybase.org>) GO Term Enrichment Tool. The colour bar represents adjusted *p*-values of significantly enriched terms.

**FIGURE 4** Wild-type (WT) and kinase-dead (KD) variants of GmMCK2 induced distinct transcriptome reprogramming in response to soybean cyst nematode (SCN) infection. (a) Venn diagram of upregulated and downregulated genes identified in root tissues of WT-GmMCK2 and KD-GmMCK2 plants at 5 days post-infection (dpi). (b) Heat map representation of significantly enriched gene ontology (GO) terms among uniquely upregulated or downregulated genes identified in root tissues of WT-GmMCK2 and KD-GmMCK2 plants at 5 dpi.



Differentially phosphorylated peptides between WT-GmMCK2 and control samples under non-infected conditions were identified using a  $p < 0.05$  with a cut-off fold-change value of 2. From this comparison, 198 unique peptides corresponding to 180 unique proteins were hyperphosphorylated in WT-GmMCK2 as compared with control samples, whereas 138 unique peptides corresponding to 123 unique proteins were hypophosphorylated (Figure 5a, Table S5). As expected the large majority of the phosphorylated residues were identified at serine (90.5%) followed by threonine (8.8%) and tyrosine (0.7%) with 85% of the differentially phosphorylated proteins containing one phosphorylation site (Figure 5b,c). Furthermore, we observed enrichment in [SP] and [LS] phosphorylation motifs among

the differentially phosphorylated peptides (Figure 5d). By comparing KD-GmMCK2 samples with those of empty vector, we identified 397 peptides corresponding to 340 proteins as hyperphosphorylated and 52 peptides corresponding to 49 proteins as hypophosphorylated (Figure 6a, Table S6). The phosphorylation sites occurred at serine (90%), threonine (9.3%) and tyrosine (0.7%) residues with 89% of the phosphopeptides containing one phosphorylation site (Figure 6b,c). The RxxS and SP phosphorylation sites were significantly over-represented among the differentially phosphorylated peptides detected from this comparison (Figure 6d).

Remarkably, the number of hyperphosphorylated peptides identified in KD-GmMCK2 samples was twice the number identified in

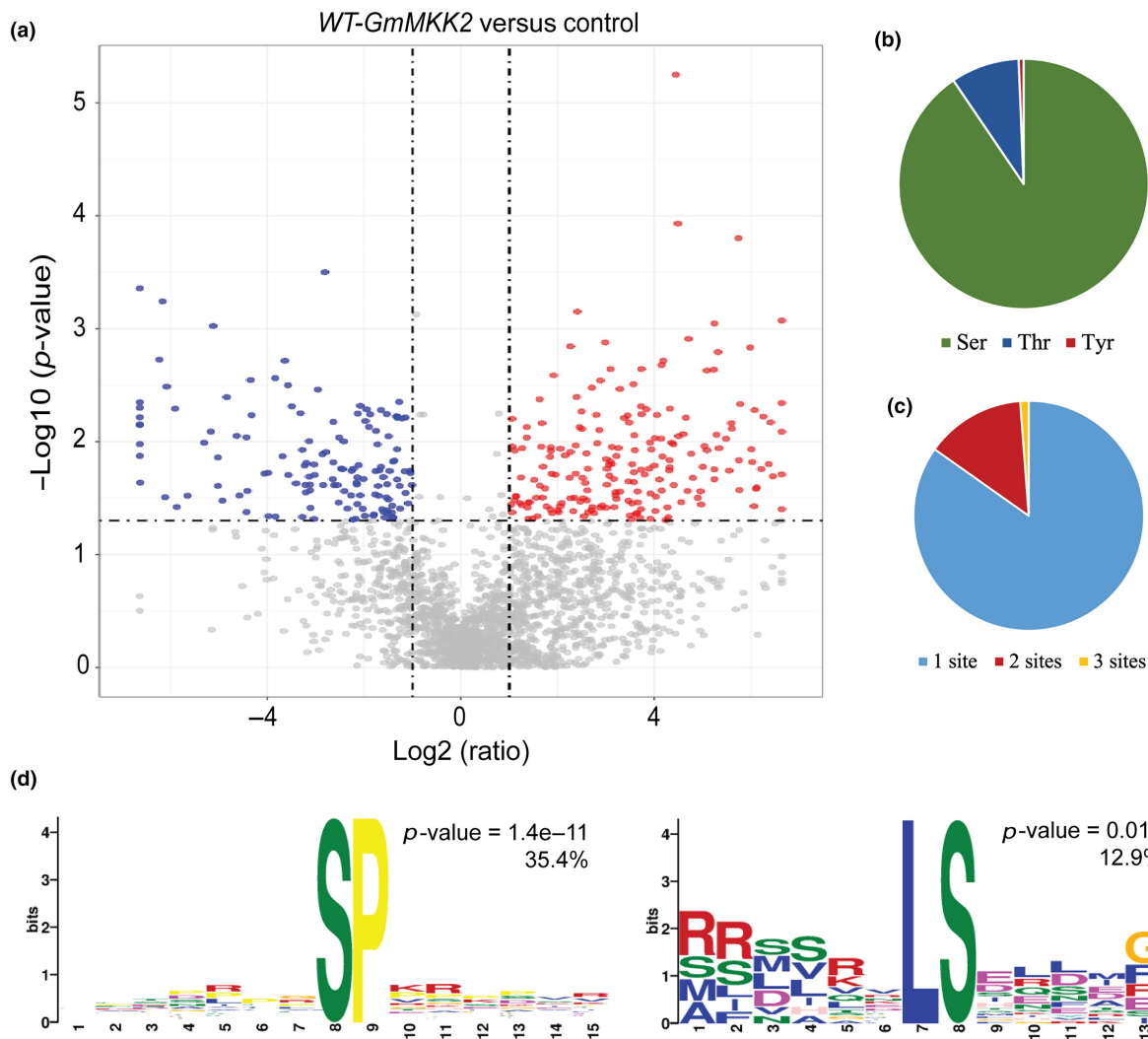


**FIGURE 5** Quantitative phosphoproteome analysis of the WT-GmMKK2 root tissues under non-infected conditions. (a) Volcano plot representation of fold-change values ( $\log_2$  scale) and significance levels ( $\log_{10}$   $p$ -value) of 336 differentially phosphorylated peptides between WT-GmMKK2 and control plants expressing the empty vector under non-infected conditions. (b) Proportion of differentially phosphorylated serine, threonine and tyrosine residues. (c) Proportion of single, double and triple phosphorylation sites in the differentially phosphorylated peptides. (d) Enrichment of SP and LS sites among the 336 differentially phosphorylated peptides. The percentage and significance ( $p$ -value) of the enriched motif among the differentially phosphorylated peptides are indicated.

WT-GmMKK2 samples (397 vs. 198). In contrast, the number of hypophosphorylated peptides in the KD-GmMKK2 samples was almost one-third of the number identified in WT-GmMKK2 samples (52 vs. 138). This finding suggests that suppressing the negative regulatory function of GmMKK2 indirectly induces phosphorylation of a significant number of proteins under non-infected conditions.

## 2.7 | Phosphoproteomic profiles of WT-GmMKK2 and KD-GmMKK2 overexpressing plants under SCN-infected conditions

We examined the extent to which GmMKK2 mediates protein phosphorylation changes in response to SCN infection. To this end, we compared SCN-infected root samples of WT-GmMKK2 overexpressing plants to non-infected samples and identified 442

differentially phosphorylated peptides (Figure 7a, Table S7). Of these differentially phosphorylated peptides, 398 corresponding to 349 proteins were more abundantly phosphorylated in SCN-infected WT-GmMKK2 samples relative to non-infected samples, whereas only 44 peptides corresponding to 42 proteins were less abundantly phosphorylated (Figure 7a, Table S7). These results indicate that upon SCN infection, WT-GmMKK2 signalling mediates protein phosphorylation to a much higher degree than dephosphorylation. The phosphorylated residues were observed at serine (87%), threonine (11%) and tyrosine (2%) residues with phosphorylation of 90% these peptides occurring at a single residue (Figure 7b,c). Only the SP phosphorylation sites were significantly over-represented among the differentially phosphorylated peptides (Figure 7d). Among the differentially phosphorylated proteins in WT-GmMKK2 after SCN infection, we found several protein kinases, including a number of MPKs, protein phosphatases



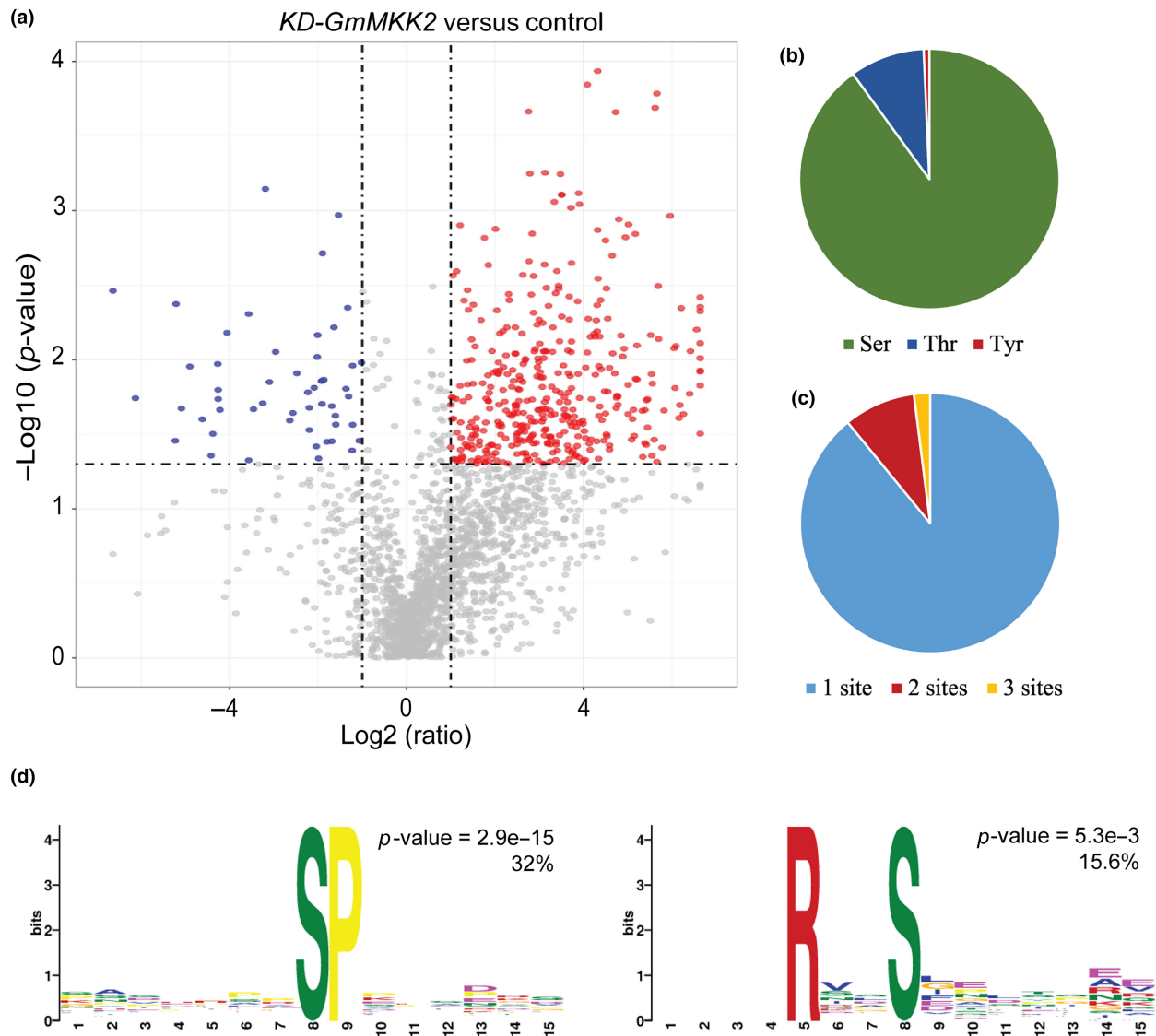


**FIGURE 6** Quantitative phosphoproteome analysis of the *KD-GmMKK2* root tissues under non-infected conditions. (a) Volcano plot representation of fold change values ( $\log_2$  scale) and significance levels ( $\log_{10} p\text{-value}$ ) of 449 differentially phosphorylated peptides between *KD-GmMKK2* and control plants expressing the empty vector under non-infected conditions. (b) Proportion of differentially phosphorylated serine, threonine and tyrosine residues. (c) Proportion of single, double and triple phosphorylation sites in the differentially phosphorylated peptides. (d) Enrichment of SP and RxxS sites among the 449 differentially phosphorylated peptides. The percentages and significance ( $p$ -values) of the enriched motifs among the differentially phosphorylated peptides are indicated.

and proteins involved in endo- and exocytosis, nuclear organization and chromatin rearrangement (Figure 7e). In addition, we identified a number of transcription and translation initiation factors (Figure 7e). Together, these findings suggest that GmMKK2 signalling is not only limited to gene transcriptional regulation but might also contribute to translation efficiency.

Similarly, we determined protein phosphorylation changes in the *KD-GmMKK2* root samples upon SCN infection in comparison with non-infected *KD-GmMKK2* samples. Sixty peptides corresponding to 58 proteins were more abundantly phosphorylated and 101 peptides corresponding to 99 proteins were less abundantly phosphorylated in SCN-infected *KD-GmMKK2* samples relative to non-infected samples (Figure 8a, Table S8). These data indicate that, unlike the

wild-type variant, the catabolically inactive isoform of *GmMKK2* contributes to protein dephosphorylation to a much higher degree than phosphorylation under SCN infection conditions. The phosphorylated residues were found at serine (90%), tyrosine (9%) and threonine (<1%) with 86% of the phosphorylated peptides showing one phosphorylated residue (Figure 8b,c). The SP phosphorylation site was significantly over-represented among the differentially phosphorylated peptides (Figure 8d). Among the differentially phosphorylated proteins, we identified several involved in protein ubiquitination, nuclear organization and chromatin remodelling (Figure 8e). Furthermore, we found a number of proteins with potential role in defence response, including several remorin proteins as well as proteins involved in the cytokinin pathway (Figure 8e).



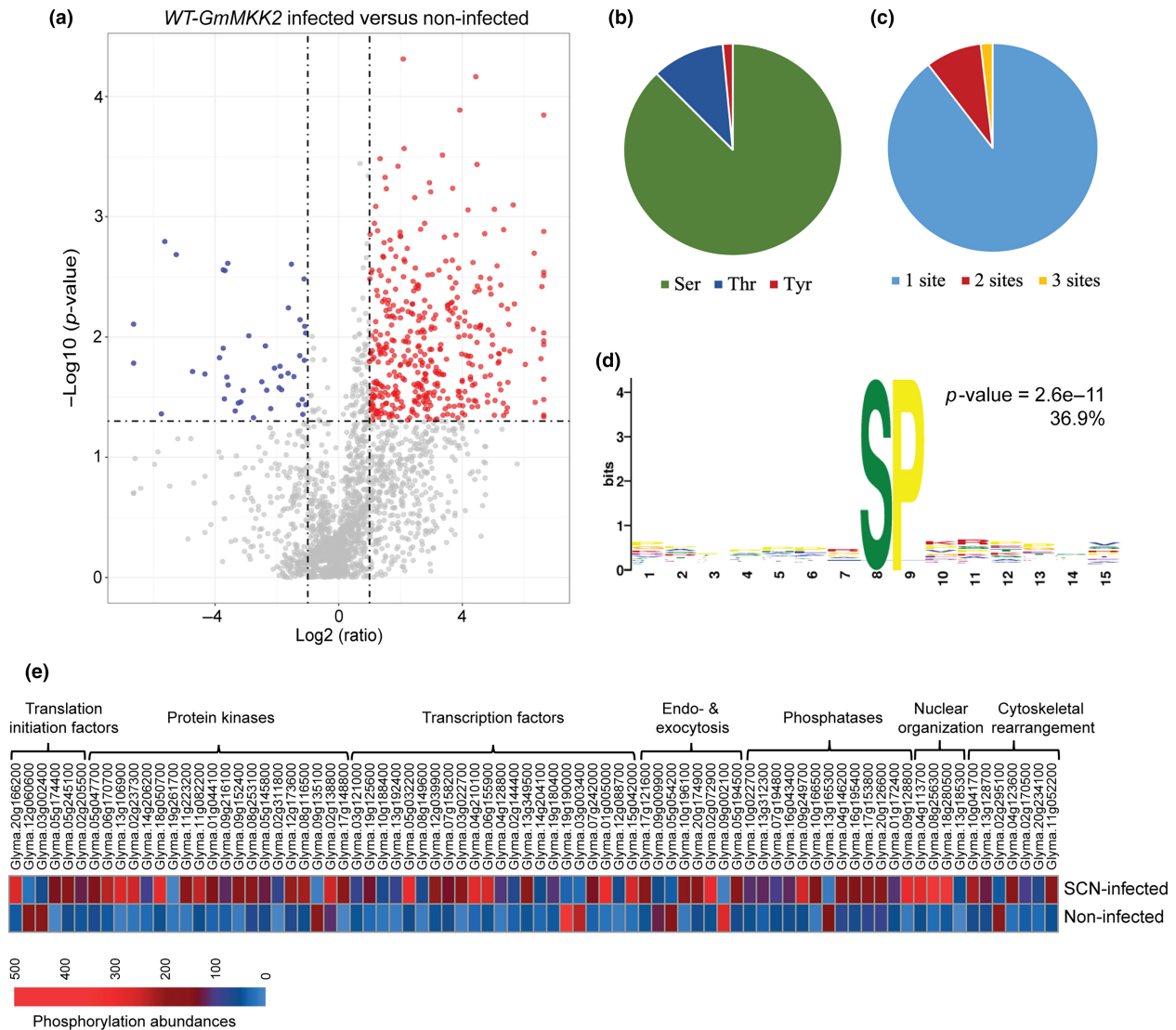


**FIGURE 7** Quantitative phosphoproteome analysis of the *WT-GmMCK2* root tissues under soybean cyst nematode (SCN)-infected conditions. (a) Volcano plot representation of fold-change values ( $\log_2$  scale) and significance levels ( $\log_{10}$   $p$ -value) of 442 differentially phosphorylated peptides between SCN-infected and non-infected root tissues of *WT-GmMCK2* plants collected at 5 days post-infection. (b) Proportion of differentially phosphorylated serine, threonine and tyrosine residues. (c) Proportion of single, double and triple phosphorylation sites in the differentially phosphorylated peptides. (d) Enrichment of SP site among the 442 differentially phosphorylated peptides. The percentage and significance ( $p$ -value) of the enriched motif among the differentially phosphorylated peptides are indicated. (e) Heatmap representation showing phosphorylation abundances of selected proteins in the *WT-GmMCK2* root samples under non-infected and SCN-infected conditions.

## 2.8 | Identification of potential direct targets of GmMCK2 under SCN infection

To identify potential direct targets of GmMCK2, we compared the hyper- and hypophosphorylated proteins identified in *KD-GmMCK2* with those identified in *WT-GmMCK2* under SCN-infected conditions. We reasoned that potential direct targets of GmMCK2 should show a significant increase in phosphopeptide abundance in *WT-GmMCK2* and/or significant decrease in *KD-GmMCK2* in response to SCN infection. By applying these two criteria, we identified 391 potential direct targets of

GmMCK2 (Table S9). These potential direct targets exhibited significant enrichment for proteins involved in nucleus organization (GO:0006997), L-proline biosynthetic process (GO:0055129) and vesicle fusion (GO:0006906). In addition, the targets included genes involved in a broad range of biological processes, including negative regulation of cellular defence response, response to oxidative stress, innate immune response, endocytosis, exocytosis, cell differentiation, transcription regulation, mRNA processing and signal transduction, among others, highlighting the complexity of the signalling networks regulated by GmMCK2 in response to SCN infection (Table S9).

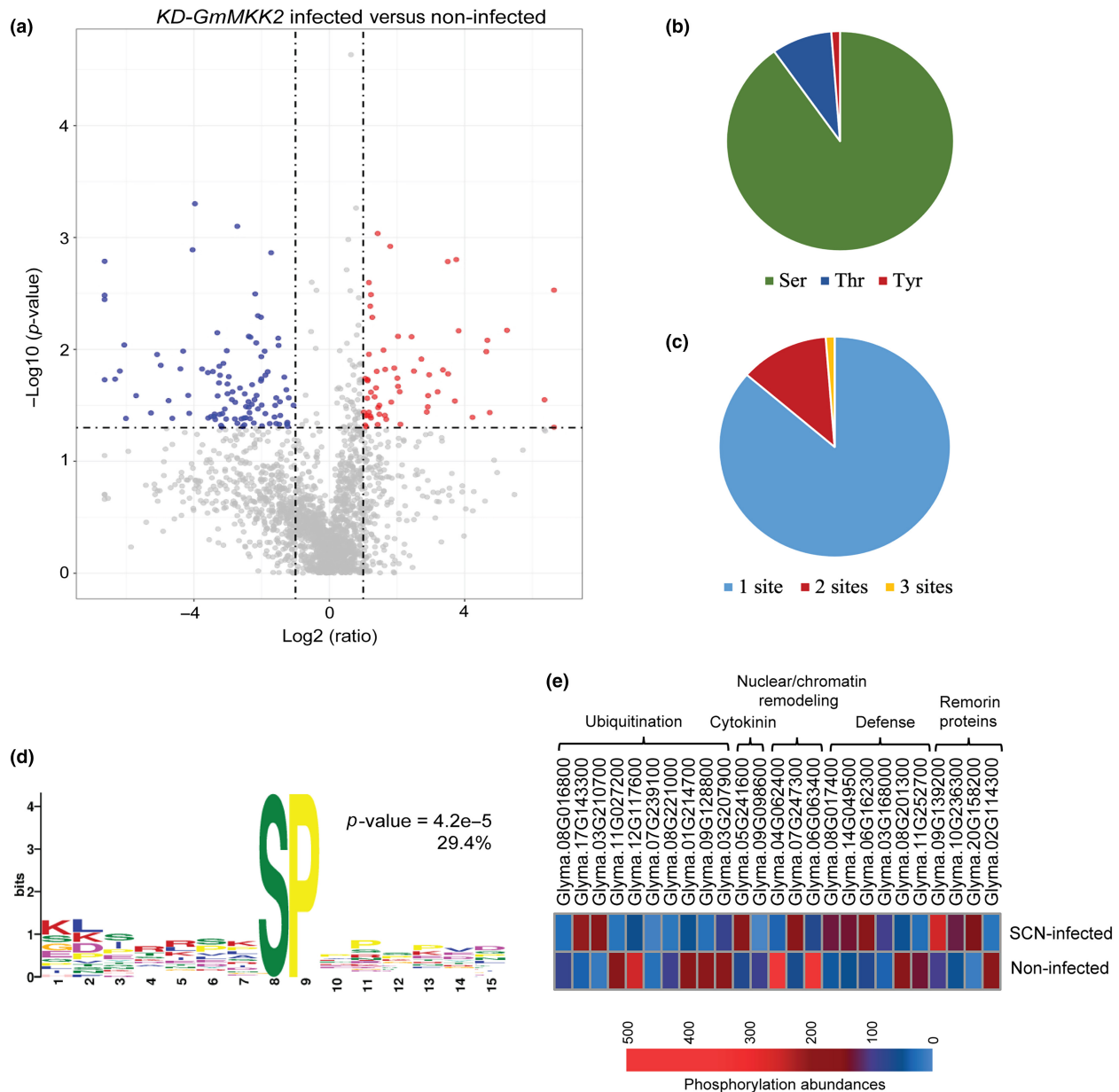


**FIGURE 8** Quantitative phosphoproteome analysis of the *KD-GmMCK2* root tissues under soybean cyst nematode (SCN)-infected conditions. (a) Volcano plot representation of fold-change values ( $\log_2$  scale) and significance levels ( $\log_{10}$   $p$ -value) of 161 differentially phosphorylated peptides between SCN-infected and non-infected root tissues of *KD-GmMCK2* plants collected at 5 days post-infection. (b) Proportion of differentially phosphorylated serine, threonine and tyrosine residues. (c) Proportion of single, double and triple phosphorylation sites in the differentially phosphorylated peptides. (d) Enrichment of SP site among the 161 differentially phosphorylated peptides. The percentage and significance ( $p$ -value) of the enriched motif among the differentially phosphorylated peptides are indicated. (e) Heatmap representation showing phosphorylation abundances of selected proteins in the *KD-GmMCK2* root samples under non-infected and SCN-infected conditions.

## 2.9 | Functional requirement of specific phosphorylation sites for soybean response to SCN infection

We examined the impact of differentially phosphorylated sites on plant susceptibility to SCN by generating phosphomimic and phospho-dead variants of two selected genes. The differentially phosphorylated serines in SUN1 (Glyma.13g185300) at positions 57, 60 and 87 were mutated to glutamate (E) and alanine

(A) to generate phosphomimic SUN1<sup>S57E/S60E/S87E</sup> and phospho-dead SUN1<sup>S57A/S60A/S87A</sup> variants, respectively. Similarly, the differentially phosphorylated serine in the transcription factor INDETERMINATE (ID)-DOMAIN 4 (IDD4, Glyma.19g180400) at position 57 was mutated to glutamate and alanine to generate phosphomimic and phospho-dead variants, IDD4<sup>S57E</sup> and IDD4<sup>S57A</sup>, respectively. Wild-type, phosphomimic and phospho-dead of both genes were overexpressed in Williams 82 using transgenic hairy roots as described above. Transgenic hairy

roots expressing the empty binary vector were used as control. Composite plants with GFP-positive roots were inoculated with SCN and cyst indices were determined 5 weeks after inoculation. Overexpression of the wild-type variant of *SUN1* showed a slight non-significant increase in cyst index, whereas overexpression of the phosphomimic *SUN1*<sup>S57E/S60E/S87E</sup> and phospho-dead *SUN1*<sup>S57A/S60A/S87A</sup> variants significantly increased soybean resistance to SCN, showing cyst index of 41.9% and 22.3%, respectively (Figure 9a,b). This result suggests that phosphorylation of S57, S60 and S87 is temporally regulated and that constitutive phosphorylation/dephosphorylation of these residues hinders nematode parasitism of soybean. Overexpression of wild-type *IDD4* and *IDD4*<sup>S57E</sup> significantly enhanced plant resistance to SCN showing, respectively, cyst index of 66% and 59% of that of control plants (Figure 9c,d). In contrast, the *IDD4*<sup>S57A</sup> overexpression showed a non-significant reduction in cyst index (Figure 9c,d), suggesting that phosphorylation of this residue contributes to plant defence signalling.

### 3 | DISCUSSION

In the present study, we report that *GmMCK2* functions as a negative regulator of plant defence response and plays an important role in establishing the interaction between soybean and SCN. Gene expression analysis revealed upregulation of *GmMCK2* during the early stage of infection (3 and 5 dpi), pointing to a role in basal defence when the syncytium is undergoing formation and patterning. The downregulation at later stages of SCN infection (7 and 10 dpi) suggests that the endogenous level of *GmMCK2* is an important determinant of soybean-SCN interactions. This suggestion was examined by overexpressing wild-type and catabolically inactive variants of *GmMCK2*. Overexpression of WT-*GmMCK2* showed a slight non-significant increase in soybean susceptibility to SCN, whereas the non-functional variant, KD-*GmMCK2*, caused a remarkable 88% reduction in plant susceptibility in comparison with control plants. These SCN susceptibility data provided the first evidence that *GmMCK2* functions as a negative regulator of defence signalling upon SCN infection of soybean.

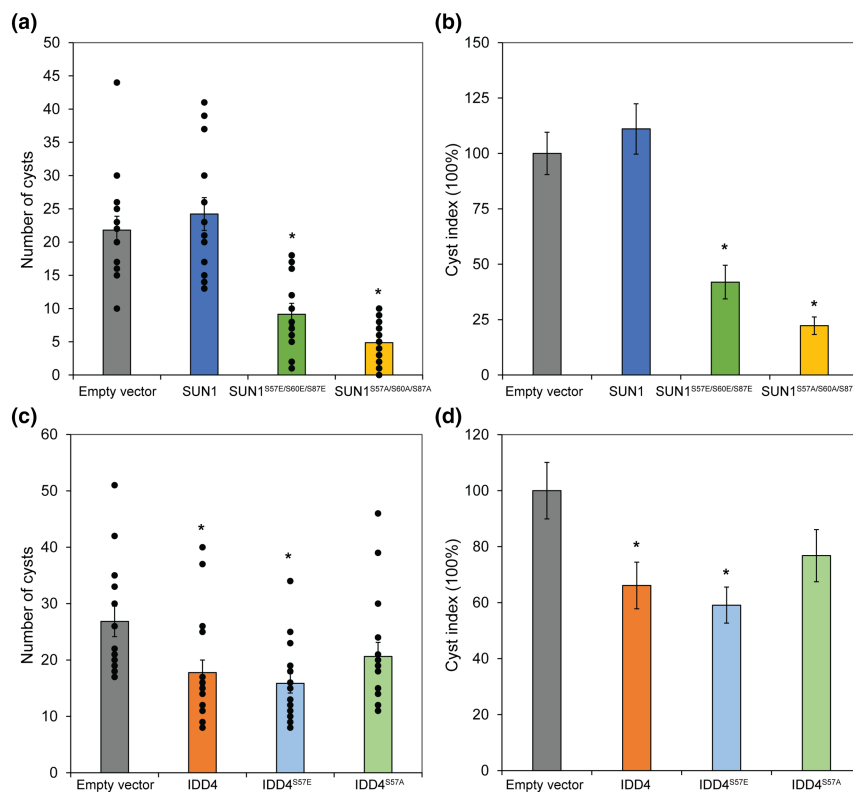


**FIGURE 9** Impact of differentially phosphorylated sites on soybean susceptibility to soybean cyst nematode (SCN). Wild-type, phosphomimic and phospho-dead variants of *SUN1* (Glyma.13g185300) and *IDD4* (Glyma.19g180400) were overexpressed in the SCN-susceptible cultivar Williams 82 using transgenic hairy root system. Transgenic hairy roots expressing the empty binary vector were similarly generated and included as control. Composite plants were inoculated with approximately 2500 eggs of SCN and 5 weeks after inoculation cysts were isolated, counted and used to calculate cyst indexes. (a, b) Cyst counts (a) and cyst indexes (b) of transgenic hairy roots overexpressing wild-type, phosphomimic (*SUN1*<sup>S57E/S60E/S87E</sup>) and phospho-dead (*SUN1*<sup>S57A/S60A/S87A</sup>) variants of *SUN1*. (c, d) Cyst counts (c) and cyst indexes (d) of transgenic hairy roots overexpressing wild-type, phosphomimic (*IDD4*<sup>S57E</sup>) and phospho-dead (*IDD4*<sup>S57A</sup>) variants of *IDD4*. Statistically significant differences between phosphomimic or phospho-dead variants and control plants were calculated using analysis of variance ( $p < 0.05$ ) and indicated with asterisks.

Our transcriptome data further supported this notion. Under non-infected conditions, overexpression of *KD-GmMKK2* resulted in dramatic upregulation of defence-related genes and downregulation of genes involved in growth and development. Similar findings were previously reported, showing that *Arabidopsis mkk1/mkk2* double mutation caused constitutive activation of defence gene expression and exhibited enhanced pathogen resistance (Gao et al., 2008; Pitzschke, Djamei, et al., 2009). However, in soybean, *GmMKK1/GmMKK2* co-silenced plants did not exhibit constitutive activation of defence signalling, a phenotype that was expected from inhibiting negative regulators of immunity (Liu et al., 2011). This was attributed to inefficient co-silencing and the possibility that other unknown MKKs function redundantly in this pathway, considering that *GmMKK1* and *GmMKK2* have several homologues in soybean (Liu et al., 2011). This limitation was probably overcome in our experiments because of the dominant-negative effect of the kinase-dead mutation that sequesters downstream targets and dampens the effects of canonical phosphorylation from redundant kinases (Hawk et al., 2023; Hewezi et al., 2015; Piya et al., 2022). In response to SCN infection, the *KD-GmMKK2* overexpression plants further augmented defence signalling, particularly those involved in response to chitin, respiratory burst and the salicylic acid-mediated signalling pathway but inhibited genes involved in cell wall modifications, nitrate transport and sugar metabolism. These results indicate that *KD-GmMKK2*-overexpressing plants were primed for SCN resistance via constitutive activation of defence signalling.

Careful examination of the differentially expressed genes identified in *WT-GmMKK2* and *KD-GmMKK2* root samples under non-infected and infected conditions provided insights into key functions of *GmMKK2*. We found several genes coding for MAPK cascade components or homologues of confirmed nuclear substrates among the differentially expressed genes. More specifically, *MPK1*, *MPK3*, *MPK4*, *MPK9*, *MPK16*, *MAPKKK4*, *MAPKKK5*, *MAPKKK14*, *MAPKKK17*, *MAPKKK18* and *MAPKKK21* exhibited differential expression patterns in *WT-GmMKK2* and/or *KD-GmMKK2* samples under infected or non-infected conditions. This finding suggests that MAPKs form complex and highly interconnected signalling cascades, most probably due to their multifaceted nature of activation, regulation and function in various aspects of plant development as well as biotic and abiotic stresses (Bigear & Hirt, 2018; Jiang et al., 2022). Of note is that several genes encoding *MAPKKK21* and *MAPK4* were downregulated in *WT-GmMKK2* but upregulated in *KD-GmMKK2* plants, implying that a feedback mechanism regulating the expression of *GmMKK2* may exist in which *MAPKKK21* and *MAPK4* function, respectively, upstream and downstream of *GmMKK2*. Another noteworthy finding is the upregulation of several genes encoding *WRKY33* and *WRKY46* only in *KD-GmMKK2* root samples in response to SCN infection. The fact that *WRKY33* and *WRKY46* are positive regulators of basal plant defence and immunity and function downstream of *MAPK3/MAPK6* (Mao et al., 2011; Sheikh et al., 2016) indicates that *GmMKK2* is involved in an intricate network of interactions

with other MAPK components transforming pathogen signals into cellular responses.

Our phosphoproteomic analysis revealed how *GmMKK2* establishes signalling modules during SCN infection. A considerable number of differentially phosphorylated proteins were determined in *KD-GmMKK2* and *WT-GmMKK2* samples under non-infected and SCN-infected conditions. In all comparisons, the SP phosphorylation site was significantly enriched among the phosphopeptides, consistent with the finding that MAPKs are proline-guided serine/threonine kinases (Bigear & Hirt, 2018). The [LS] and [RxxS] phosphorylation sites were also significantly over-represented among the phosphopeptides detected in non-infected *WT-GmMKK2* and *KD-GmMKK2* samples, respectively (Figures 5d and 6d), pointing to the involvement of other mechanisms in regulating substrate selection for phosphorylation.

Phosphoproteomic profiling of *WT-GmMKK2* and *KD-GmMKK2* under non-infected and SCN-infected conditions revealed distinct patterns of phosphorylation changes. While 88% of the phosphorylation changes mediated by *KD-GmMKK2* under non-infected conditions were hyperphosphorylated, only 37% of the differentially phosphorylated peptides were hyperphosphorylated under infected conditions. The opposite trend was observed in the *WT-GmMKK2* samples with 41% and 90% of the differentially phosphorylated peptides being hyperphosphorylated under non-infected and SCN-infected conditions, respectively. These findings imply that suppressing the negative regulatory function of *GmMKK2* indirectly induces phosphorylation of a significant number of proteins under non-infected conditions and that the wild-type variant became more active in phosphorylating target proteins in response to SCN infection.

Our phosphoproteomic analyses resulted in the identification of 391 potential targets of *GmMKK2* under SCN infection. These potential targets are involved in a broad range of biological processes, demonstrating the complex signalling networks in which *GmMKK2* functions to facilitate the likelihood of SCN infection. A striking finding of our results is the enrichment of proteins functioning in nuclear organization and structure among the *GmMKK2* putative targets. This includes, for instance, homologues of *Arabidopsis* little nuclei1 (Glyma.08g256300 and Glyma.18g280500), *SAD1/UNC-84* domain protein 1 (*SUN1*, Glyma.13g185300; and Glyma.15G223100) and *WPP* domain interacting protein 1 (*WIP1*, Glyma.04g113700). The finding that these proteins form a complex and play a key role in nuclear shape and structure (Graumann et al., 2014; Oda & Fukuda, 2011; Zhou et al., 2015) suggests a role of *GmMKK2*-mediated phosphorylation of these proteins in their assembly and/or function. Given that nuclei undergo many rounds of endoreduplication and become enlarged/elongated during syncytium formation (De Almeida Engler & Gheysen, 2013; de Almeida-Engler et al., 1999; Ohtsu et al., 2017), we speculated that phosphorylation of these proteins may contribute to syncytium formation and thus plant susceptibility to SCN. This speculation was further reinforced by our data showing that overexpression of the phosphomimic

SUN1<sup>S57E/S60E/S87E</sup> and phospho-dead SUN1<sup>S57A/S60A/S87A</sup> variants significantly reduced soybean susceptibility to SCN (Figure 9a,b).

A remarkable outcome of our analysis is the over-representation of proteins implicated in vesicle fusion among the GmMCK2 target substrates. Interestingly, these proteins (Glyma.02G195300, Glyma.02G195400, Glyma.10G082500, Glyma.17G236900, Glyma.02G072900, Glyma.02G291600 and Glyma.16G091900) belong to the syntaxin vesicular transport receptors of the t-SNARE (soluble N-ethylmaleimide-sensitive-factor attachment protein receptor) family. Syntaxins are primarily localized to the plasma membrane and participate in exocytosis and defence response (Kalde et al., 2007; Kwon et al., 2008; Pratelli et al., 2004; Robatzek, 2007). Several lines of evidence point to the involvement of syntaxins in SCN–soybean interactions. Overexpression of syntaxin38 significantly enhanced soybean resistance to SCN (Pant et al., 2014). In addition, a SNARE-like protein from SCN was found to interact with the *Rhg1*  $\alpha$ -SNAP and might function as an avirulence protein (Bekal et al., 2015). More recently, it has been shown that two soybean syntaxin proteins interact with the *Rhg1*  $\alpha$ -SNAP protein and contribute to SCN resistance (Dong et al., 2020), further supporting the association between the vesicle trafficking pathway and SCN resistance. Considering the enrichment of syntaxin proteins among the GmMCK2 target substrates together with their implications in SCN resistance, it is conceivable to suggest a role of MCK2 in diversifying defence signalling upon SCN infection through regulation of membrane dynamics and exocytosis.

The GmMCK2 putative substrates included several transcription factors and translation initiation factors. Among the transcription factors, we found several AT-HOOK MOTIF NUCLEAR LOCALIZED (AHL) proteins, homeobox domain-containing proteins, basic-leucine zipper (bZIP) and INDETERMINATE DOMAIN (IDD) factors, for instance. IDD proteins are highly conserved among plants and play multiple roles in plant growth and development as well as innate immunity (Kumar et al., 2019; Völz, Kim, Mi, Mariappan, et al., 2019). One of the IDD proteins, IDD4, is a coordinator of plant growth and basal immunity in *Arabidopsis* (Völz, Kim, Mi, Rawat, et al., 2019). *Arabidopsis* IDD4 is phosphorylated and activated by MPK6 at a conserved serine residue (Bethke et al., 2009; Mao et al., 2011; Völz, Kim, Mi, Rawat, et al., 2019), which was also detected in *WT-GmMCK2* samples upon SCN infection. Our analysis revealed that, unlike the IDD4 phospho-dead mutant, the wild-type and IDD4 phospho-mimicking variants significantly reduced soybean susceptibility to SCN (Figure 9c,d), implying a profound biological impact of phosphorylation status of this residue on defence signalling. The identification of various translation initiation factors among the putative targets suggests that GmMCK2 exerts a powerful impact not only on gene expression but also on protein synthesis upon SCN infection. Notably, MPK6 was also identified as differentially phosphorylated in *WT-GmMCK2* upon SCN infection.

Taken together, our data show that GmMCK2 phosphorylates various signalling molecules as well as transcriptional and translational regulators, pointing to the presence of signalling shortcuts in addition to the canonical MAPK cascades to initiate downstream signalling networks that ultimately regulate gene expression and translation initiation.

A substantial number of proteins involved in ubiquitination, epigenetic modifications, the cytokinin pathway and defence response were also identified as putative substrates for GmMCK2. It is intriguing to observe that numerous proteins involved in protein ubiquitination are among the GmMCK2 targets (Table S9). The interplay between phosphorylation and ubiquitination is a well-known phenomenon in which phosphorylation generally impacts the ubiquitination and hence degradation of the targeted proteins (Hunter, 2007), which might influence soybean–SCN interactions. In addition, our finding that several chromatin remodelling factors are among the identified putative substrates shows how the activity of GmMCK2 could induce intricate post-translational modifications of phosphorylation, ubiquitination and epigenetic modifications, which have been shown to impact plant response to cyst nematodes (Bennett et al., 2022; Chronis et al., 2013; Diaz-Granados et al., 2020; Hewezi, 2020; Hewezi et al., 2015; Kud et al., 2019).

Notably, the type-B response regulator 12 (ARR12) was among the putative targets. Previous studies have documented the importance of cytokinin signalling for successful feeding site formation and plant susceptibility (Shanks et al., 2016; Siddique et al., 2015). ARR12 is a positive regulator of cytokinin signalling and phosphorylation of the type-B ARRs activates their DNA-binding domain, resulting in transcriptional activation of cytokinin-responsive genes (Argueso et al., 2010; Hwang & Sheen, 2001). Thus, it is reasonable to speculate that reduced phosphorylation of ARR12 in *KD-GmMCK2* samples upon SCN infection would interrupt transcriptional activation of cytokinin-responsive genes leading to the observed enhanced SCN resistance.

Other putative targets with defence- and immunity-related functions include, for example, the soybean homologues of *Arabidopsis* MEMBRANE ATTACK COMPLEX/PERFORIN-LIKE 1 (MACP1, Glyma.11G252700), which is involved in salicylic acid accumulation and programmed cell death in response to pathogen infection (Zhang et al., 2022); the pleiotropic drug resistance transporters PDR12 (Glyma.13G361900) and PEN3 (Glyma.08G201300), which function redundantly in the secretion of the phytoalexin camalexin (He et al., 2019); and RESPIRATORY BURST OXIDASE HOMOLOG D (RBOHD, Glyma.04G203200), which is believed to be the primary source of ROS during PTI and plays an essential role in plant immunity (Kadota et al., 2015; O'Brien et al., 2012) and plant–nematode interactions (Chopra et al., 2021; Siddique et al., 2014; Teixeira et al., 2016). However, further studies are needed to determine how phosphorylation status of these proteins induces functional changes leading to specific response to SCN infection.



## 4 | EXPERIMENTAL PROCEDURES

### 4.1 | Determining the subcellular localization of WT-GmMKK2 and KD-GmMKK2

In order to generate a kinase-inactive variant of MKK2, KD-GmMKK2, the conserved lysine 99 and 194 at the ATP and substrate-binding sites, respectively, were mutated to arginine, as described previously by Hawk et al. (2023), Hewezi et al. (2015), and Piya et al. (2022). Both the kinase-inactive and wild-type variants were synthesized and PCR-amplified using forward and reverse primers containing the attB1 and attB2 sequences, respectively (Table S10). PCR-amplified fragments were cloned into the Gateway vector pDONR221 (ThermoFisher Scientific) using BP clonase. The donor clones were then used for C-terminal fusion with enhanced cyan fluorescent protein (eCFP) in the pGWB444 vector (Addgene 74830) using LR clonase to generate expression clones. The expression clones were transformed into *Agrobacterium tumefaciens* EHA105, which used to infiltrate *Nicotiana benthamiana* leaves as previously described by Burch-Smith et al. (2007). Imaging CFP signal was performed 24 h post-infiltration on a confocal microscope using a 40× water immersion objective lens and a 25-mW argon laser.

### 4.2 | Generation of composite soybean plants overexpressing WT-GmMKK2 and KD-GmMKK2

The coding sequences of KD-GmMKK2 and WT-GmMKK2 were synthesized and cloned into pG2RNAi2 vector under the control of the soybean ubiquitin promoter by swapping the  $\beta$ -glucuronidase gene (*GUS*) using gene-specific primers sites (Table S10). Similarly, wild-type, phosphomimic and phospho-dead variants of *SUN1* (*Glyma.13g185300*) and *IDD4* (*Glyma.19g180400*) were synthesized and cloned in the pG2RNAi2 vector using forward and reverse primers containing, respectively, the *AscI* and *AvrII* recognition sites (Table S10). Serines in *SUN1* at position 57, 60 and 87 were mutated to glutamate (E) and alanine (A) to generate phosphomimic and phospho-dead variants, respectively. Similarly, the differentially phosphorylated serine in *IDD4* at position 57 was mutated to glutamate and alanine to generate phosphomimic and phospho-dead variants, respectively. Soybean transgenic hairy roots were generated following the protocol outlined by Kereszt et al. (2007). Constructed vectors or the empty vector containing the GFP reporter gene were introduced into *Agrobacterium rhizogenes* K599 and injected into the hypocotyl of 5-day-old Williams 82 seedlings. Approximately 3 weeks after injection, transgenic roots were identified using a dissecting microscope furnished with a GFP filter. Overexpression level of *GmMKK2* was further confirmed in four biological samples of transgenic hairy roots using RT-qPCR, as described below.

### 4.3 | Nematode infection assays

Composite soybean plants with transgenic hairy roots overexpressing WT-GmMKK2, KD-GmMKK2 as well as wild-type, phosphomimic and phospho-dead variants of *SUN1* (*Glyma.13g185300*) and *IDD4* (*Glyma.19g180400*) or the empty vector were planted in pots containing a 3:1 ratio of sand to soil. Susceptibility assays were conducted with 15 replicates per construct and organized in a randomized complete block design in the greenhouse. Each plant was inoculated with approximately 2500 SCN Hg Type 0 (race 3) eggs. Cysts were extracted from each plant individually 5 weeks after inoculation and counted. The number of cysts on each experimental group was compared to the control plants expressing the empty vector. Cyst index was calculated for each gene by dividing the average number of cysts in each experimental group to the control and multiplying by 100. Statistically significant differences were calculated between experimental groups and the control using a mixed model analysis of variance in SAS (Glimmix procedure, SAS institute) with  $p < 0.05$ .

### 4.4 | RNA extraction and RT-qPCR analysis

To quantify the expression level of *GmMKK2* in response to SCN infection, 4-day-old Williams 82 seedlings were germinated in germination paper and inoculated with approximately 300s-stage SCN Hg Type 0 juveniles or 0.1% agarose (mock). At 3, 5, 7 and 14 dpi, syncytium-enriched tissues were dissected and collected from infected roots. Meanwhile, whole roots were collected from non-infected plants and used as control samples. Three biological replicates of syncytium-enriched root tissues and the corresponding non-infected roots were collected at each time point. Total RNA was isolated according to Verwoerd et al. (1989). RNA was DNase-treated and diluted to a concentration of 25 ng/ $\mu$ L for RT-qPCR quantification. RT-qPCR was performed using Verso SYBR green 1-step (Thermo Fisher Scientific) on a QuantStudio 6 Flex Real-Time PCR System (Applied Biosystems). The PCR cycle of 60°C for 90s and 72°C for 30s was repeated 40 times. Dissociation curves were generated from PCR-amplified products with a slow gradient from 50 to 95°C. Both *ubiquitin* (*Glyma.20G141600*) and  $\beta$ -*actin* (*Glyma.15G050200*) were used as reference genes to normalize *GmMKK2* expression levels (Rambani et al., 2015, 2020; Wan et al., 2015).

### 4.5 | RNA-sequencing library preparation and analysis

Composite plant with transgenic hairy roots overexpressing WT-GmMKK2, KD-GmMKK2, or empty vector (control) were inoculated with 300 J2s of SCN HG type 0. Three biological replicates were

collected for each treatment group at 5 dpi. Total RNA extraction was done using hot phenol as described previously and mRNA was isolated using oligo(dT) beads (Thermo Fisher Scientific). Non-stranded, non-directional mRNA libraries were prepared, multiplexed and sequenced using the Illumina NovaSeq 6000 platform with 150bp paired-end reads. After removing low quality reads using TRIMMOMATIC v. 0.39 (Bolger et al., 2014), high-quality reads obtained from trimming were mapped to the Williams 82 soybean genome (Wm82.a4.v1) using STAR (v. 2.5.0) (Dobin et al., 2013). Uniquely mapped reads were counted using HTSeq (Anders et al., 2015), then normalized and finally used to identify differentially expressed genes using the DESeq2 package (Love et al., 2014) in R Studio with a false discovery rate (FDR) < 5% and 2-fold change cut-off.

#### 4.6 | Protein extraction and liquid chromatography-mass spectrometry

Total protein was extracted from 150–200mg of the same root samples used for RNA-seq analysis. Ground and lyophilized tissue samples were lysed with Type 4 Protein Extraction Reagent and Protease Inhibitor Cocktail (Sigma-Aldrich) following the manufacturer's guidelines. Protein was precipitated with a cold 1:1 acetone and methanol mixture followed by centrifugation. Pelleted protein was air dried and suspended in ammonium bicarbonate (50mM) and concentrations were measured with the bicinchoninic acid (BCA) protein assay (Thermo Fisher Scientific). Samples were then reduced, alkylated and digested with trypsin. Digested products were acidified with trifluoroacetic acid (TFA) and extracted with Sep-Pak C18 solid phase extraction cartridge (Waters), following the manufacturer's guidelines. The functional magnetic microparticles MagReSyn ZrO<sub>2</sub> and Zr-IMAC (ReSyn Biosciences) were used for phosphopeptide enrichment. Liquid chromatography-mass spectrometry (LC-MS) was used to analyse the samples. A Dionex RSLC nano HPLC and Orbitrap Fusion Lumos mass spectrometer (Thermo Fisher Scientific) with a 2h gradient and a 75 μm × 50cm PepMap C18 column (Thermo Fisher Scientific) were used to identify peptides.

#### 4.7 | Quantitative phosphoproteomic data analysis

The Uniprot soybean protein database (Proteome ID: UP000008827) was used for peptide mapping and quantification using Proteome Discoverer 2.4 (Thermo Fisher Scientific) and Sequest HT algorithm (Eng et al., 1994) following the parameters previously described by Hawk et al. (2023). Dynamic phosphorylation sites for the enriched dataset were considered at serine, threonine and tyrosine residues. The precursor mass ranged from 350 to 5000Da and tolerance parameters for fragment and precursor mass were set to 0.6Da and 10ppm, respectively. Low abundance resampling method was used to substitute missing values and abundances were normalized

relative to the total peptide abundances. Analysis of variance and mean separation with Tukey's post hoc analysis were used to determine significantly differentially enriched peptides and proteins in each comparison. Additionally, statistically differentially phosphorylated peptides were determined using  $p < 0.05$  and 1.5-fold change cut-off. Data visualization were performed using the R packages ggplot2 (Ito & Murphy, 2013) and pheatmap (Kolde, 2015).

#### ACKNOWLEDGEMENTS

This project was supported by funds from the Agriculture and Food Research Initiative competitive grant no. 2018-67013-27822 from the USDA National Institute of Food and Agriculture to T.H. We also would like to thank the Proteomics & Mass Spectrometry Facility at the Danforth Plant Science Center for phosphoproteome analysis and several undergraduate students in the Hewezi laboratory for technical assistance.

#### CONFLICT OF INTEREST STATEMENT

The authors declare that there are no conflicts of interest.

#### DATA AVAILABILITY STATEMENT

RNA-seq data described in this study were submitted to the NCBI database at [www.ncbi.nlm.nih.gov/genbank/](http://www.ncbi.nlm.nih.gov/genbank/), Gene Expression Omnibus under accession number GSE232688.

#### ORCID

Tarek Hewezi  <https://orcid.org/0000-0001-5256-8878>

#### REFERENCES

- de Almeida-Engler, J., De Vleeschauwer, V., Burssens, S., Celenza, J.L., Inzé, D., Van Montagu, M. et al. (1999) Molecular markers and cell cycle inhibitors show the importance of cell cycle progression in nematode-induced galls and syncytia. *The Plant Cell*, 11, 793–807.
- Anders, S., Pyl, P.T. & Huber, W. (2015) HTSeq—a Python framework to work with high-throughput sequencing data. *Bioinformatics*, 31, 166–169.
- Argueso, C.T., Raines, T. & Kieber, J.J. (2010) Cytokinin signaling and transcriptional networks. *Current Opinion in Plant Biology*, 13, 533–539.
- Asai, T., Tena, G., Plotnikova, J., Willmann, M.R., Chiu, W.-L., Gomez-Gomez, L. et al. (2002) MAP kinase signalling cascade in *Arabidopsis* innate immunity. *Nature*, 415, 977–983.
- Bekal, S., Domier, L.L., Gonfa, B., Lakhssassi, N., Meksem, K. & Lambert, K.N. (2015) A SNARE-like protein and biotin are implicated in soybean cyst nematode virulence. *PLoS One*, 10, e0145601.
- Bennett, M., Piya, S., Baum, T.J. & Hewezi, T. (2022) miR778 mediates gene expression, histone modification, and DNA methylation during cyst nematode parasitism. *Plant Physiology*, 189, 2432–2453.
- Berriri, S., Garcia, A.V., dit Frey, N.F., Rozhon, W., Pateyron, S., Leonhardt, N. et al. (2012) Constitutively active mitogen-activated protein kinase versions reveal functions of *Arabidopsis* MPK4 in pathogen defense signaling. *The Plant Cell*, 24, 4281–4293.
- Bethke, G., Unthan, T., Uhrig, J.F., Pöschl, Y., Gust, A.A., Scheel, D. et al. (2009) Flg22 regulates the release of an ethylene response factor substrate from MAP kinase 6 in *Arabidopsis thaliana* via ethylene signaling. *Proceedings of the National Academy of Sciences of the United States of America*, 106, 8067–8072.
- Bigeard, J. & Hirt, H. (2018) Nuclear signaling of plant MAPKs. *Frontiers in Plant Science*, 9, 469.

- Bolger, A.M., Lohse, M. & Usadel, B. (2014) Trimmomatic: a flexible trimmer for illumina sequence data. *Bioinformatics*, 30, 2114–2120.
- Brader, G., Djamei, A., Teige, M., Palva, E.T. & Hirt, H. (2007) The MAP kinase MKK2 affects disease resistance in *Arabidopsis*. *Molecular Plant-Microbe Interactions*, 20, 589–596.
- Brodersen, P., Petersen, M., Bjørn Nielsen, H., Zhu, S., Newman, M.A., Shokat, K.M. et al. (2006) *Arabidopsis* MAP kinase 4 regulates salicylic acid- and jasmonic acid/ethylene-dependent responses via EDS1 and PAD4. *The Plant Journal*, 47, 532–546.
- Burch-Smith, T.M., Schiff, M., Caplan, J.L., Tsao, J., Czymmek, K. & Dinesh-Kumar, S.P. (2007) A novel role for the TIR domain in association with pathogen-derived elicitors. *PLoS Biology*, 5, e68.
- Chopra, D., Hasan, M.S., Matera, C., Chitambo, O., Mendy, B., Mahlitz, S.V. et al. (2021) Plant parasitic cyst nematodes redirect host indole metabolism via NADPH oxidase-mediated ROS to promote infection. *New Phytologist*, 232, 318–331.
- Chronis, D., Chen, S., Lu, S., Hewezi, T., Carpenter, S.C.D., Loria, R. et al. (2013) A ubiquitin carboxyl extension protein secreted from a plant-parasitic nematode *Globodera rostochiensis* is cleaved in planta to promote plant parasitism. *The Plant Journal*, 74, 185–196.
- De Almeida Engler, J. & Gheysen, G. (2013) Nematode-induced endoreduplication in plant host cells: why and how? *Molecular Plant-Microbe Interactions*, 26, 17–24.
- Diaz-Granados, A., Sterken, M.G., Overmars, H., Ariaans, R., Holterman, M., Pokhare, S.S. et al. (2020) The effector GpRbp-1 of *Globodera pallida* targets a nuclear HECT E3 ubiquitin ligase to modulate gene expression in the host. *Molecular Plant Pathology*, 21, 66–82.
- Dobin, A., Davis, C.A., Schlesinger, F., Drenkow, J., Zaleski, C., Jha, S. et al. (2013) STAR: ultrafast universal RNA-seq aligner. *Bioinformatics*, 29, 15–21.
- Dong, J., Zielinski, R.E. & Hudson, M.E. (2020) T-SNAREs bind the Rhg1  $\alpha$ -SNAP and mediate soybean cyst nematode resistance. *The Plant Journal*, 104, 318–331.
- Eng, J.K., McCormack, A.L. & Yates, J.R. (1994) An approach to correlate tandem mass spectral data of peptides with amino acid sequences in a protein database. *Journal of the American Society for Mass Spectrometry*, 5, 976–989.
- Gao, M., Liu, J., Bi, D., Zhang, Z., Cheng, F., Chen, S. et al. (2008) MEK1, MKK1/MKK2 and MPK4 function together in a mitogen-activated protein kinase cascade to regulate innate immunity in plants. *Cell Research*, 18, 1190–1198.
- Graumann, K., Vanrobays, E., Tutois, S., Probst, A.V., Evans, D.E. & Tatout, C. (2014) Characterization of two distinct subfamilies of SUN-domain proteins in *Arabidopsis* and their interactions with the novel KASH-domain protein AtTIK. *Journal of Experimental Botany*, 65, 6499–6512.
- Hamel, L.P., Nicole, M.C., Sritubtim, S., Morency, M.J., Ellis, M., Ehltling, J. et al. (2006) Ancient signals: comparative genomics of plant MAPK and MAPKK gene families. *Trends in Plant Science*, 11, 192–198.
- Hammes, U.Z., Schachtman, D.P., Berg, R.H., Nielsen, E., Koch, W., McIntyre, L.M. et al. (2005) Nematode-induced changes of transporter gene expression in *Arabidopsis* roots. *Molecular Plant-Microbe Interactions*, 18, 1247–1257.
- Hawk, T.E., Piya, S., Zadegan, S.B., Li, P., Rice, J.H. & Hewezi, T. (2023) The soybean immune receptor GmBIR1 regulates host transcriptome, spliceome, and immunity during cyst nematode infection. *New Phytologist*, 239, 2335–2352.
- He, X., Wang, C., Wang, H., Li, L. & Wang, C. (2020) The function of MAPK cascades in response to various stresses in horticultural plants. *Frontiers in Plant Science*, 11, 952.
- He, Y., Xu, J., Wang, X., He, X., Wang, Y., Zhou, J. et al. (2019) The *Arabidopsis* pleiotropic drug resistance transporters PEN3 and PDR12 mediate camalexin secretion for resistance to *Botrytis cinerea*. *The Plant Cell*, 31, 2206–2222.
- He, Z., Webster, S. & He, S.Y. (2022) Growth-defense trade-offs in plants. *Current Biology*, 32, R634–R639.
- Hewezi, T. (2020) Epigenetic mechanisms in nematode-plant interactions. *Annual Review of Phytopathology*, 58, 119–138.
- Hewezi, T. & Baum, T.J. (2017) Communication of sedentary plant-parasitic nematodes with their host plants. *Advances in Botanical Research*, 82, 305–324.
- Hewezi, T., Juvale, P.S., Piya, S., Maier, T.R., Rambani, A., Rice, J.H. et al. (2015) The cyst nematode effector protein 10A07 targets and recruits host posttranslational machinery to mediate its nuclear trafficking and to promote parasitism in *Arabidopsis*. *The Plant Cell*, 27, 891–907.
- Hunter, T. (2007) The age of crosstalk: phosphorylation, ubiquitination, and beyond. *Molecular Cell*, 28, 730–738.
- Hwang, I. & Sheen, J. (2001) Two-component circuitry in *Arabidopsis* cytokinin signal transduction. *Nature*, 413, 383–389.
- Ichimura, K., Casais, C., Peck, S.C., Shinozaki, K. & Shirasu, K. (2006) MEK1 is required for MPK4 activation and regulates tissue-specific and temperature-dependent cell death in *Arabidopsis*. *Journal of Biological Chemistry*, 281, 36969–36976.
- Ito, K. & Murphy, D. (2013) Application of ggplot2 to pharmacometric graphics. *CPT: Pharmacometrics & Systems Pharmacology*, 2, e79.
- Jiang, M., Zhang, Y., Li, P., Jian, J., Zhao, C. & Wen, G. (2022) Mitogen-activated protein kinase and substrate identification in plant growth and development. *International Journal of Molecular Sciences*, 23, 2744.
- Kadota, Y., Shirasu, K. & Zipfel, C. (2015) Regulation of the NADPH oxidase RBOHD during plant immunity. *Plant and Cell Physiology*, 56, 1472–1480.
- Kalde, M., Nühse, T.S., Findlay, K. & Peck, S.C. (2007) The syntaxin SYP132 contributes to plant resistance against bacteria and secretion of pathogenesis-related protein 1. *Proceedings of the National Academy of Sciences of the United States of America*, 104, 11850–11855.
- Kereszt, A., Li, D., Indrasumunar, A., Nguyen, C.D., Nontachaiyapoom, S., Kinkema, M. et al. (2007) *Agrobacterium rhizogenes*-mediated transformation of soybean to study root biology. *Nature Protocols*, 2, 948–952.
- Kolde, R. (2015) *Pheatmap: pretty heatmaps*. R package v.1.0.8. Available from: <https://rdrr.io/cran/pheatmap/> [Accessed 10th February 2023].
- Kud, J., Wang, W., Gross, R., Fan, Y., Huang, L., Yuan, Y. et al. (2019) The potato cyst nematode effector RHA1B is a ubiquitin ligase and uses two distinct mechanisms to suppress plant immune signaling. *PLoS Pathogens*, 15, e1007720.
- Kumar, M., Le, D.T., Hwang, S., Seo, P.J. & Kim, H.U. (2019) Role of the indeterminate domain genes in plants. *International Journal of Molecular Sciences*, 20, 2286.
- Kwon, C., Neu, C., Pajonk, S., Yun, H.S., Lipka, U., Humphry, M. et al. (2008) Co-option of a default secretory pathway for plant immune responses. *Nature*, 451, 835–840.
- Kyndt, T., Vieira, P., Gheysen, G. & de Almeida-Engler, J. (2013) Nematode feeding sites: unique organs in plant roots. *Planta*, 238, 807–818.
- Li, J., Deng, F., Wang, H., Qiang, X., Meng, Y. & Shan, W. (2022) The Raf-like kinase Raf36 negatively regulates plant resistance against the oomycete pathogen *Phytophthora parasitica* by targeting MKK2. *Molecular Plant Pathology*, 23, 530–542.
- Liu, J.Z., Horstman, H.D., Braun, E., Graham, M.A., Zhang, C., Navarre, D. et al. (2011) Soybean homologs of MPK4 negatively regulate defense responses and positively regulate growth and development. *Plant Physiology*, 157, 1363–1378.
- Liu, Y., Huang, X., Li, M., He, P. & Zhang, Y. (2016) Loss-of-function of *Arabidopsis* receptor-like kinase BIR1 activates cell death and defense responses mediated by BAK1 and SOBIR1. *New Phytologist*, 212, 637–645.
- Love, M.I., Huber, W. & Anders, S. (2014) Moderated estimation of fold change and dispersion for RNA-seq data with DESeq2. *Genome Biology*, 15, 550.

- Mao, G., Meng, X., Liu, Y., Zheng, Z., Chen, Z. & Zhang, S. (2011) Phosphorylation of a WRKY transcription factor by two pathogen-responsive MAPKs drives phytoalexin biosynthesis in *Arabidopsis*. *The Plant Cell*, 23, 1639–1653.
- Mejias, J., Truong, N.M., Abad, P., Favery, B. & Quentin, M. (2019) Plant proteins and processes targeted by parasitic nematode effectors. *Frontiers in Plant Science*, 10, 970.
- Mendy, B., Wang'ombe, M.W., Radakovic, Z.S., Holbein, J., Ilyas, M., Chopra, D. et al. (2017) *Arabidopsis* leucine-rich repeat receptor-like kinase NLR1 is required for induction of innate immunity to parasitic nematodes. *PLoS Pathogens*, 13, e1006284.
- Meng, X. & Zhang, S. (2013) MAPK cascades in plant disease resistance signaling. *Annual Review of Phytopathology*, 51, 245–266.
- Moustafa, K., AbuQamar, S., Jarrar, M., Al-Rajab, A.J. & Trémouillaux-Guiller, J. (2014) MAPK cascades and major abiotic stresses. *Plant Cell Reports*, 33, 1217–1225.
- Nakagami, H., Soukupová, H., Schikora, A., Zárský, V. & Hirt, H. (2006) A mitogen-activated protein kinase kinase kinase mediates reactive oxygen species homeostasis in *Arabidopsis*. *Journal of Biological Chemistry*, 281, 38697–38704.
- O'Brien, J.A., Daudi, A., Butt, V.S. & Paul Bolwell, G. (2012) Reactive oxygen species and their role in plant defence and cell wall metabolism. *Planta*, 236, 765–779.
- Oda, Y. & Fukuda, H. (2011) Dynamics of *Arabidopsis* SUN proteins during mitosis and their involvement in nuclear shaping. *The Plant Journal*, 66, 629–641.
- Ohtsu, M., Sato, Y., Kurihara, D., Suzaki, T., Kawaguchi, M., Maruyama, D. et al. (2017) Spatiotemporal deep imaging of syncytium induced by the soybean cyst nematode *Heterodera glycines*. *Protoplasma*, 254, 2107–2115.
- Pant, S.R., Matsye, P.D., McNeece, B.T., Sharma, K., Krishnavajhala, A., Lawrence, G.W. et al. (2014) Syntaxin 31 functions in *Glycine max* resistance to the plant parasitic nematode *Heterodera glycines*. *Plant Molecular Biology*, 85, 107–121.
- Park, H.C., Park, B.O., Kim, H.S., Kim, S.H., Lee, S.W. & Chung, W.S. (2021) AtMPK6-induced phosphorylation of AtERF72 enhances its DNA binding activity and interaction with TGA4/OBF4 in *Arabidopsis*. *Plant Biology*, 23, 11–20.
- Petersen, M., Brodersen, P., Naested, H., Andreasson, E., Lindhart, U., Johansen, B. et al. (2000) *Arabidopsis* MAP kinase 4 negatively regulates systemic acquired resistance. *Cell*, 103, 1111–1120.
- Pitzschke, A., Djamei, A., Bitton, F. & Hirt, H. (2009) A major role of the MEKK1–MKK1/2–MPK4 pathway in ROS signalling. *Molecular Plant*, 2, 120–137.
- Pitzschke, A., Schikora, A. & Hirt, H. (2009) MAPK cascade signalling networks in plant defence. *Current Opinion in Plant Biology*, 12, 421–426.
- Piya, S., Hawk, T., Patel, B., Baldwin, L., Rice, J.H., Stewart, C.N., Jr. et al. (2022) Kinase-dead mutation: a novel strategy for improving soybean resistance to soybean cyst nematode *Heterodera glycines*. *Molecular Plant Pathology*, 23, 417–430.
- Piya, S., Kihm, C., Rice, J.H., Baum, T.J. & Hewezi, T. (2017) Cooperative regulatory functions of miR858 and MYB83 during cyst nematode parasitism. *Plant Physiology*, 174, 1897–1912.
- Pratelli, R., Sutter, J.U. & Blatt, M.R. (2004) A new catch in the SNARE. *Trends in Plant Science*, 9, 187–195.
- Qiu, J.-L., Zhou, L., Yun, B.-W., Nielsen, H.B., Fiil, B.K., Petersen, K. et al. (2008) *Arabidopsis* mitogen-activated protein kinase kinases MKK1 and MKK2 have overlapping functions in defense signaling mediated by MEKK1, MPK4, and MKS1. *Plant Physiology*, 148, 212–222.
- Rambani, A., Hu, Y., Piya, S., Long, M., Rice, J.H., Pantalone, V. et al. (2020) Identification of differentially methylated miRNA genes during compatible and incompatible interactions between soybean and soybean cyst nematode. *Molecular Plant–Microbe Interactions*, 33, 1340–1352.
- Rambani, A., Rice, J.H., Liu, J., Lane, T., Ranjan, P., Mazarei, M. et al. (2015) The methylome of soybean roots during the compatible interaction with the soybean cyst nematode. *Plant Physiology*, 168, 1364–1377.
- Robatzek, S. (2007) Vesicle trafficking in plant immune responses. *Cellular Microbiology*, 9, 1–8.
- Rodriguez, M.C., Petersen, M. & Mundy, J. (2010) Mitogen-activated protein kinase signaling in plants. *Annual Reviews in Plant Biology*, 61, 621–649.
- Shanks, C.M., Rice, J.H., Zubo, Y., Schaller, G.E., Hewezi, T. & Kieber, J.J. (2016) The role of cytokinin during infection of *Arabidopsis thaliana* by the cyst nematode *Heterodera schachtii*. *Molecular Plant–Microbe Interactions*, 29, 57–68.
- Sheikh, A.H., Eschen-Lippold, L., Pecher, P., Hoehenwarter, W., Sinha, A.K., Scheel, D. et al. (2016) Regulation of WRKY46 transcription factor function by mitogen-activated protein kinases in *Arabidopsis thaliana*. *Frontiers in Plant Science*, 7, 61.
- Siddique, S., Coomer, A., Baum, T. & Williamson, V.M. (2022) Recognition and response in plant–nematode interactions. *Annual Review of Phytopathology*, 60, 143–162.
- Siddique, S. & Grundler, F.M. (2015) Metabolism in nematode feeding sites. *Advances in Botanical Research*, 73, 119–138.
- Siddique, S. & Grundler, F.M. (2018) Parasitic nematodes manipulate plant development to establish feeding sites. *Current Opinion in Microbiology*, 46, 102–108.
- Siddique, S., Matera, C., Zs, R., Shamim Hasan, M., Gutbrod, P., Rozanska, E. et al. (2014) Parasitic worms stimulate host NADPH oxidases to produce reactive oxygen species that limit plant cell death and promote infection. *Science Signalling*, 7, ra33.
- Siddique, S., Radakovic, Z.S., De La Torre, C.M., Chronis, D., Novák, O., Ramireddy, E. et al. (2015) A parasitic nematode releases cytokinin that controls cell division and orchestrates feeding site formation in host plants. *Proceedings of the National Academy of Sciences of the United States of America*, 112, 12669–12674.
- Sidonskaya, E., Schweighofer, A., Shubchynskyy, V., Kammerhofer, N., Hofmann, J., Wiczorek, K. et al. (2016) Plant resistance against the parasitic nematode *Heterodera schachtii* is mediated by MPK3 and MPK6 kinases, which are controlled by the MAPK phosphatase AP2C1 in *Arabidopsis*. *Journal of Experimental Botany*, 67, 107–118.
- Smant, G., Helder, J. & Govers, A. (2018) Parallel adaptations and common host cell responses enabling feeding of obligate and facultative plant parasitic nematodes. *The Plant Journal*, 93, 686–702.
- Sobczak, M. & Golinowski, W. (2011) Cyst nematodes in syncytia. In: Jones, J., Fenoll, C. & Gheysen, G. (Eds.) *Genomics and molecular genetics of plant–nematode interactions*. New York, NY: Springer, pp. 61–83.
- Suarez-Rodriguez, M.C., Adams-Phillips, L., Liu, Y., Wang, H., Su, S.-H., Jester, P.J. et al. (2006) MEKK1 is required for flg22-induced MPK4 activation in *Arabidopsis* plants. *Plant Physiology*, 143, 661–669.
- Takagi, M., Hamano, K., Takagi, H., Morimoto, T., Akimitsu, K., Terauchi, R. et al. (2018) Disruption of the MAMP-induced MEKK1–MKK1/MKK2–MPK4 pathway activates the TNL immune receptor SMN1/RPS6. *Plant and Cell Physiology*, 60, 778–787.
- Teixeira, M.A., Wei, L. & Kaloshian, I. (2016) Root-knot nematodes induce pattern-triggered immunity in *Arabidopsis thaliana* roots. *New Phytologist*, 211, 276–287.
- Tena, G., Asai, T., Chiu, W.-L. & Sheen, J. (2001) Plant mitogen-activated protein kinase signaling cascades. *Current Opinion in Plant Biology*, 4, 392–400.
- Tena, G., Boudsocq, M. & Sheen, J. (2011) Protein kinase signaling networks in plant innate immunity. *Current Opinion in Plant Biology*, 14, 519–529.
- Verwoerd, T.C., Dekker, B.M. & Hoekema, A. (1989) A small-scale procedure for the rapid isolation of plant RNAs. *Nucleic Acids Research*, 17, 2362.
- Völz, R., Harris, W., Hirt, H. & Lee, Y.-H. (2022) ROS homeostasis mediated by MPK4 and SUMM2 determines synergid cell death. *Nature Communications*, 13, 1746.



- Völz, R., Kim, S.K., Mi, J., Mariappan, K.G., Siodmak, A., Al-Babili, S. et al. (2019) A chimeric IDD4 repressor constitutively induces immunity in *Arabidopsis* via the modulation of salicylic acid and jasmonic acid homeostasis. *Plant and Cell Physiology*, 60, 1536–1555.
- Völz, R., Kim, S.-K., Mi, J., Rawat, A.A., Veluchamy, A., Mariappan, K.G. et al. (2019) Indeterminate-domain 4 (IDD4) coordinates immune responses with plant-growth in *Arabidopsis thaliana*. *PLoS Pathogens*, 15, e1007499.
- Wan, J., Vuong, T., Jiao, Y., Joshi, T., Zhang, H., Xu, D. et al. (2015) Whole-genome gene expression profiling revealed genes and pathways potentially involved in regulating interactions of soybean with cyst nematode (*Heterodera glycines* Ichinohe). *BMC Genomics*, 16, 148.
- Widmann, C., Gibson, S., Jarpe, M.B. & Johnson, G.L. (1999) Mitogen-activated protein kinase: conservation of a three-kinase module from yeast to human. *Physiological Reviews*, 79, 143–180.
- Withers, J. & Dong, X. (2017) Post-translational regulation of plant immunity. *Current Opinion in Plant Biology*, 38, 124–132.
- Wu, C.-H., Abd-El-Halim, A., Bozkurt, T.O., Belhaj, K., Terauchi, R., Vossen, J.H. et al. (2017) NLR network mediates immunity to diverse plant pathogens. *Proceedings of the National Academy of Sciences of the United States of America*, 114, 8113–8118.
- Xu, H.Y., Zhang, C., Li, Z.C., Wang, Z.R., Jiang, X.X., Shi, Y.F. et al. (2018) The MAPK kinase kinase GmMEKK1 regulates cell death and defense responses. *Plant Physiology*, 178, 907–922.
- Xu, J., Meng, J., Meng, X., Zhao, Y., Liu, J., Sun, T. et al. (2016) Pathogen-responsive MPK3 and MPK6 reprogram the biosynthesis of indole glucosinolates and their derivatives in *Arabidopsis* immunity. *The Plant Cell*, 28, 1144–1162.
- Zhang, M., Su, J., Zhang, Y., Xu, J. & Zhang, S. (2018) Conveying endogenous and exogenous signals: MAPK cascades in plant growth and defense. *Current Opinion in Plant Biology*, 45, 1–10.
- Zhang, X., Dai, Y.-S., Wang, Y.-X., Su, Z.-Z., Yu, L.-J., Zhang, Z.-F. et al. (2022) Overexpression of the *Arabidopsis* MACPF protein AtMACP2 promotes pathogen resistance by activating SA signaling. *International Journal of Molecular Sciences*, 23, 8784.
- Zhang, Z., Liu, Y., Huang, H., Gao, M., Wu, D., Kong, Q. et al. (2017) The NLR protein SUMM2 senses the disruption of an immune signaling MAP kinase cascade via CRCK3. *EMBO Reports*, 18, 292–302.
- Zhang, Z., Wu, Y., Gao, M., Zhang, J., Kong, Q., Liu, Y. et al. (2012) Disruption of PAMP-induced MAP kinase cascade by a *Pseudomonas syringae* effector activates plant immunity mediated by the NB-LRR protein SUMM2. *Cell Host & Microbe*, 11, 253–263.
- Zhou, X., Graumann, K. & Meier, I. (2015) The plant nuclear envelope as a multifunctional platform LINCed by SUN and KASH. *Journal of Experimental Botany*, 66, 1649–1659.
- Zou, M., Guo, M., Zhou, Z., Wang, B., Pan, Q., Li, J. et al. (2021) MPK3- And MPK6-mediated VLN3 phosphorylation regulates Actin dynamics during stomatal immunity in *Arabidopsis*. *Nature Communications*, 12, 6474.
- Zhou, J.-M. & Zhang, Y. (2020) Plant immunity: danger perception and signaling. *Cell*, 181, 978–989.

## SUPPORTING INFORMATION

Additional supporting information can be found online in the Supporting Information section at the end of this article.

**How to cite this article:** Hawk, T.E., Piya, S., Sultana, M.S., Zadegan, S.B., Shipp, S., Coffey, N. et al. (2024) Soybean MKK2 establishes intricate signalling pathways to regulate soybean response to cyst nematode infection. *Molecular Plant Pathology*, 25, e13461. Available from: <https://doi.org/10.1111/mpp.13461>